

# Greedy Heuristics for Sampling-based Motion Planning in High-Dimensional State Spaces

Phone Thiha Kyaw<sup>1</sup>, Anh Vu Le<sup>2</sup>, Lim Yi<sup>1</sup>, Prabakaran Veerajagadheswar<sup>1</sup>, Mohan Rajesh Elara<sup>1</sup>, Dinh Tung Vo<sup>3</sup> and Minh Bui Vu<sup>4</sup>

## Abstract

Sampling-based motion planning algorithms are very effective at finding solutions in high-dimensional continuous state spaces as they do not require prior approximations of the problem domain compared to traditional discrete graph-based searches. The anytime version of the Rapidly-exploring Random Trees (RRT) algorithm, denoted as RRT\*, often finds high-quality solutions by incrementally approximating and searching the problem domain through random sampling. However, due to its low sampling efficiency and slow convergence rate, research has proposed many variants of RRT\*, incorporating different heuristics and sampling strategies to overcome the constraints in complex planning problems. Yet, these approaches address specific convergence aspects of RRT\* limitations, leaving a need for a sampling-based algorithm that can quickly find better solutions in complex high-dimensional state spaces with a faster convergence rate for practical motion planning applications.

This article unifies and leverages the greedy search and heuristic techniques used in various RRT\* variants to develop a greedy version of the anytime Rapidly-exploring Random Trees algorithm, denoted as Greedy RRT\* (G-RRT\*). It improves the initial solution-finding time of RRT\* by maintaining two trees rooted at both the start and goal ends, advancing toward each other using greedy connection heuristics. It also accelerates the convergence rate of RRT\* by introducing a greedy version of direct informed sampling procedure, which guides the sampling towards the promising region of the problem domain based on heuristics. We validate our approach on simulated planning problems, manipulation problems on Barrett WAM Arms, and on a self-reconfigurable robot, Panthera. Results show that G-RRT\* produces asymptotically optimal solution paths and outperforms state-of-the-art RRT\* variants, especially in high-dimensional planning problems.

## Keywords

Sampling-based path planning, Optimal path planning, Informed sampling, Bidirectional search, Greedy heuristics, High-dimensional planning, Reconfigurable robotic

## 1 Introduction

Robot path planning determines a collision-free geometric path from an initial state to a goal state while considering some specific optimizing objectives such as energy or distance travelled (LaValle 2006). It is a fundamental research area in robotics and many efforts have been made to develop a wide variety of path planning techniques including graph-based searches, artificial potential fields and sampling-based methods (Elbanhawi and Simic 2014). Unfortunately, it is challenging to find collision-free and optimal paths, especially in continuous search spaces or in high dimensions, and this task is generally known to be a PSPACE-hard computational problem (Reif 1979).

In order to achieve computational efficiency in high-dimensional continuous state spaces, sampling-based planning algorithms have been proposed, such as probabilistic roadmaps (PRM; Kavraki et al. 1996) and Rapidly-Exploring Random Trees (RRT; LaValle and Kuffner Jr 2001). Compared to traditional complete graph-search approaches such as Dijkstra's algorithm (Dijkstra et al. 1959) or A\* (Hart et al. 1968), these sampling-based algorithms relax the completeness requirements and find feasible solutions faster

in continuous state spaces with *probabilistic completeness* guarantees, i.e., the probability that the algorithm fails to find the solution, if one exists, decays to zero as the number of samples approaches infinity. Additionally, extensions have been developed to propose *anytime* favor sampling-based approaches such as PRM\* and RRT\* (Karaman and Frazzoli 2011), which not only hold probabilistic completeness guarantees and also have *asymptotic optimality* property, i.e., the

<sup>1</sup>ROAR Lab, Engineering Product Development, Singapore University of Technology and Design, Singapore

<sup>2</sup>Communication and Signal Processing Research Group, Faculty of Electrical and Electronics Engineering, Ton Duc Thang University, Ho Chi Minh City, Vietnam

<sup>3</sup>HUTECH Institute of Engineering, HUTECH University, Ho Chi Minh City, Vietnam

<sup>4</sup>Faculty of Engineering and Technology, Nguyen Tat Thanh University, Ho Chi Minh City, Vietnam

### Corresponding author:

Anh Vu Le, Communication and Signal Processing Research Group, Faculty of Electrical and Electronics Engineering, Ton Duc Thang University, Ho Chi Minh City, Vietnam.

Email: leanhvu@tdtu.edu.vn

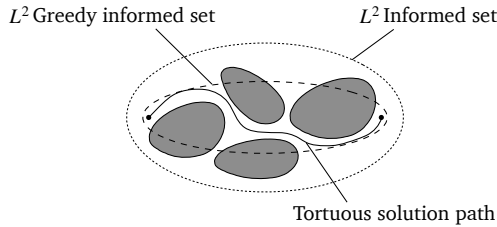


**Figure 1.** Comparison between relative sizes of the informed sets in planning problems with tortuous solution paths. The  $L^2$  informed set is estimated based on the current solution cost, therefore, having the larger ellipsoidal area. The  $L^2$  greedy informed set, on the other hand, only uses the heuristic cost of the state in the current solution with maximum admissible heuristics, thereby reducing the size of the hyperellipsoid.

algorithm almost-surely converges towards the optimum as the number of samples approaches infinity.

These anytime sampling-based algorithms are very effective to find optimal solutions on high-dimensional continuous path planning problems. Like RRTs, these approaches rely on random sampling to explore the search over the problem domain (i.e., incrementally expanding the tree through a free space). Unlike RRTs, they extend it by locally optimizing every added vertex (i.e., incrementally rewire the tree during the tree expansion process). This rewiring process makes sure RRT\* to asymptotically converge to the optimal solution if enough time is given. However, it is inefficient to rely on random sampling approach especially in large problem domains or high-dimensional state spaces since a lot of computational effort has been wasted on the states that cannot contribute to improve the current solution or exploring into unnecessary regions of the planning domain.

Therefore, several techniques have been investigated to develop extended versions of RRT and RRT\*-based algorithms. Ferguson and Stentz (2006) propose an anytime version of RRT by reusing information from previous trees to improve the quality of the current tree and solution path within the allocated time. They realized that limiting the nodes with a lower cost bound to the previous solution cost can increase the probability of finding even better solutions. Such similar sample rejection ideas have been integrated with RRT\* to further improve the convergence rate towards the optimum (Akgun and Stilman 2011; Otte and Correll 2013). Building upon these concepts, Gammell et al. (2014, 2018) introduced the direct informed sampling technique in their Informed RRT\* algorithm, which exploits the current solution path to focus the search only on promising regions of the planning domain for improving the convergence rate of RRT\*.

Informed RRT\* limits the exploration space of RRT\* by directly sampling within a hyperellipsoid determined by the current path cost. This approach indeed outperforms RRT\* in terms of convergence rate and final solution quality while maintaining a uniform sample distribution over the informed subset for optimal guarantees. However, the initial solution paths found by the planner might be tortuous, containing a large number of redundant states. Consequently, this results in unnecessarily larger informed sets, slowing down

the exploration and convergence process of the algorithm, especially in high dimensions.

This article addresses the computational burden associated with the informed hyperellipsoid proposed in Informed RRT\* by introducing a new direct informed sampling procedure. Our approach biases the sampling based on the heuristic information of the states in the current solution path, regardless of the cost, thus mitigating the impact of tortuous initial solution paths. Specifically, we propose a *greedy informed set*, a subset of the informed set, which greedily exploits the information from the current solution path to rapidly reduce the size of the informed exploration hyperellipsoid, enhancing sampling efficiency (Figure 1).

Applying direct informed sampling techniques to RRT\* does indeed improve the convergence rate of the algorithm, as the search is only focused within hyperellipsoids. However, in certain planning scenarios where the initial path takes longer to find, the advantages of focused search become impractical. One way to find faster initial solutions is to use a bidirectional approach. Bidirectional versions of RRT such as RRT-Connect (Kuffner and LaValle 2000) grows two trees, one rooted in the start and one in the goal, to explore the problem state space and uses a greedy connect heuristic to guide the trees towards each other. Therefore, this article improves the efficiency of initial solution time in planners that use focused sampling techniques by incorporating bidirectional search concepts.

Expanding upon these greedy heuristics, this paper presents Greedy RRT\* (G-RRT\*), an almost-surely asymptotically optimal sampling-based planning algorithm based on bidirectional search. G-RRT\* is presented to demonstrate the benefits of employing greedy search and heuristic techniques in sampling-based planning to achieve practical performance in high-dimensional state spaces. It shows the importance of exploiting search space to improve sample efficiency through the use of a greedy informed set. Additionally, it presents the necessity of maintaining dual rapidly exploring trees in high-dimensional planning to avoid getting stuck in local minima and to quickly find initial solutions (Figure 2).

The benefits of exploiting the problem state space with greedy heuristics are demonstrated through simulated planning problems in  $\mathbb{R}^2$ ,  $\mathbb{R}^4$ ,  $\mathbb{R}^8$  and  $\mathbb{R}^{16}$ , manipulation problems on Barrett WAM Arms in  $\mathbb{R}^{14}$ , as well as on a robotic platform, Panthera,—a 5-degree-of-freedom self-reconfigurable mobile robot (Hayat et al. 2019)—in Section 6. All planning problems are tested with the objective of minimizing path length. These experiments show that our approach is capable of finding quick initial solutions with a faster convergence rate and outperforms state-of-the-art methods, particularly in scenarios involving large planning domains.

## 1.1 Statement of contributions

This article presents the following specific contributions:

- Proposes a  $L^2$  *greedy informed set* which is constructed based on the heuristic information of the current solution path to accelerate the sampling process (Section 3).
- Presents Greedy RRT\* (G-RRT\*), a bi-directional asymptotically optimal sampling-based planning algorithm, as

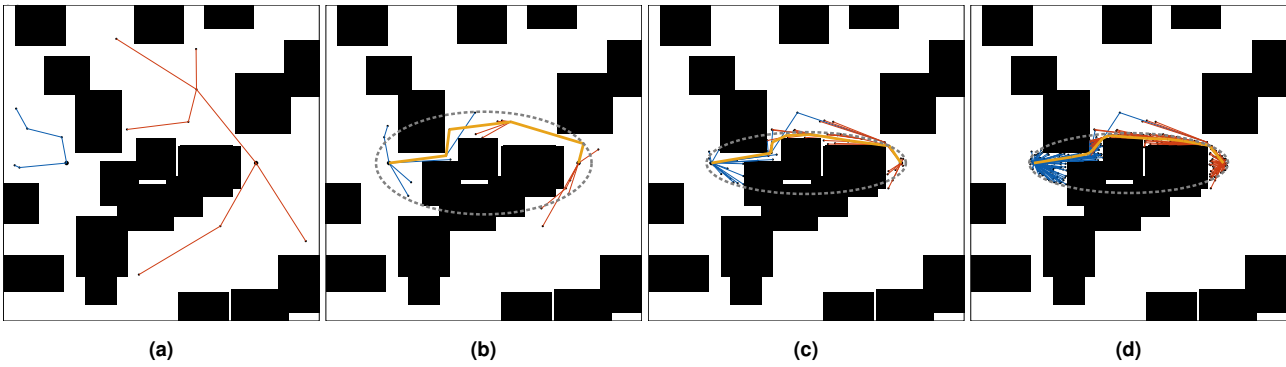


**Figure 2.** Illustrations of the progress of sampling-based bi-directional search performed by the G-RRT\* algorithm. The initial and goal states are represented by big black dots, whereas the sampled states are represented by small black dots. The start and goal trees constructed to explore the state space are shown in blue and orange, respectively, while the current solution is highlighted in yellow. The set of states that could produce better solution costs than the heuristic cost of the greedily chosen state in the current solution (the  $L^2$  greedy informed set) is highlighted with gray dashed lines. G-RRT\* starts the exploration of the problem domain by maintaining two rapidly growing trees, one rooted in the initial state and one in the goal state (a). The expansion of these two trees is guided by a greedy connection heuristic, leading towards each other to form an initial solution (b). The search then only focuses on the states that are inside the greedy informed set defined by the current solution path, improving the accuracy with more focused sampled states (c). G-RRT\* repeats these steps within the available time budget and almost-surely asymptotically converges towards the optimal solution (d).

an extension of RRT\* that leverages on these greedy heuristic concepts (Section 4).

- Proves the completeness and asymptotic optimality of G-RRT\* by building upon findings from the sampling-based planning literature (Section 5).
- Demonstrates experimentally that the benefits of greedy exploitation in large planning domains yield better success and convergence rates than state-of-the-art algorithms through simulations and real-world robotic platform (Section 6).

This article is organized as follows. Section 2 describes a path planning problem definition and provides an overview of the sampling-based path planning and background on accelerating RRT\* convergence through sampling. Section 3 defines the greedy informed set, which is demonstrated with a G-RRT\* algorithm in Section 4. Section 5 analyses the theoretical guarantees of G-RRT\*. Section 6 examines and demonstrates G-RRT\* in simulations and in real-world experiments with a self-reconfigurable robot, Panthera. Finally, the article concludes with a discussion and future research plans in Section 7.

## 2 Preliminaries and Background

This section first presents a formal definition of the optimal path planning problem (Section 2.1) and then reviews an existing literature on sampling-based planning algorithms (Section 2.2) and accelerating convergence of these asymptotically optimal planners based on distribution of samples in the state space (Section 2.3).

### 2.1 Problem Formulation

In robotics, the path planning problem is commonly distinguished into two problems namely: *feasible* and *optimal* planning (Karaman and Frazzoli 2011). The feasible path planning finds a collision-free geometric path from

an initial location to a target location. Therefore, there are many possible solutions in feasible planning problems. The optimal path planning, on the other hand, finds a best unique feasible path based on the given optimization objective. The following definitions given in Definition 1 and 2 formally describes the feasible and optimal path planning problems.

**Definition 1.** (The feasible path planning problem). *Let  $\mathcal{X} \in \mathbb{R}^n$  be the state space of the geometric planning problem. Let  $\mathcal{X}_{obs} \subseteq \mathcal{X}$  be the set of all states,  $\mathbf{x}$ , that are in collision with obstacles,  $\mathcal{O}$ , and  $\mathcal{X}_{free} = \mathcal{X} \setminus \mathcal{X}_{obs}$  be the resultant collision-free set. Let  $\mathbf{x}_I \in \mathcal{X}_{free}$  be the initial state and  $\mathbf{x}_G \in \mathcal{X}_{free}$  be the goal state. Let  $\pi : [0, 1] \rightarrow \mathcal{X}_{free}$  be a feasible path in continuous domain and  $\Sigma$  be the set of all non-trivial solution paths. The feasible path planning problem is then formally defined as to find any path  $\pi' \in \Sigma$  in (1) from this set that connects  $\mathbf{x}_I$  to  $\mathbf{x}_G$  through collision-free space,*

$$\pi' \in \left\{ \pi \in \Sigma \mid \pi(0) = \mathbf{x}_I, \pi(1) = \mathbf{x}_G, \forall s \in [0, 1], \pi(s) \in \mathcal{X}_{free} \right\}. \quad (1)$$

**Definition 2.** (The optimal path planning problem). *Let  $\mathcal{X} \in \mathbb{R}^n$  be the state space of the geometric planning problem. Let  $\mathcal{X}_{obs} \subseteq \mathcal{X}$  be the set of all states,  $\mathbf{x}$ , that are in collision with obstacles,  $\mathcal{O}$ , and  $\mathcal{X}_{free} = \mathcal{X} \setminus \mathcal{X}_{obs}$  be the resultant collision-free set. Let  $\mathbf{x}_I \in \mathcal{X}_{free}$  be the initial state and  $\mathbf{x}_G \in \mathcal{X}_{free}$  be the goal state. Let  $\pi : [0, 1] \rightarrow \mathcal{X}_{free}$  be a feasible path in continuous domain. The optimal path planning problem is then formally defined as to find a feasible path  $\pi^*$  in (2) from  $\mathbf{x}_I$  to  $\mathbf{x}_G$  through collision-free space that minimizes the given cost objective,  $c : \Sigma \rightarrow \mathbb{R}_{\geq 0}$ ,*

$$\pi^* = \arg \min_{\pi \in \Sigma} \left\{ c(\pi) \mid \pi(0) = \mathbf{x}_I, \pi(1) = \mathbf{x}_G, \forall s \in [0, 1], \pi(s) \in \mathcal{X}_{free} \right\}, \quad (2)$$

where  $\Sigma$  denotes the set of all non-trivial paths and  $\mathbb{R}_{\geq 0}$  is the set of non-negative real numbers.

Formal guarantees provided by sampling-based algorithms concerning these feasible or optimal planning problems are often probabilistic in nature. An algorithm is considered to be *probabilistically complete* (Definition 3) when, given an infinite number of samples, the probability of finding a solution, should one exist, approaches one. Furthermore, it is described as *almost-surely asymptotically optimal* (Definition 4), if the same algorithm, with an increasing number of samples, converges asymptotically to the optimum with a probability of one, provided that an optimal solution exists (Karaman and Frazzoli 2011). Note that almost-sure asymptotic optimality implies probabilistic completeness.

**Definition 3.** (Probabilistic completeness). *A sampling-based path planning algorithm is said to be probabilistically complete if, as the number of samples approaches infinity, the probability of finding a feasible solution (Definition 1) converges to one,*

$$\liminf_{n \rightarrow \infty} \mathbb{P}(\pi_n \in \Sigma, \pi_n(0) = \mathbf{x}_I, \pi_n(1) = \mathbf{x}_G) = 1, \quad (3)$$

where  $n$  is the number of samples and  $\pi_n$  is the path from the initial state to the goal state found by the algorithm from those samples.

**Definition 4.** (Almost-sure asymptotic optimality). *A sampling-based path planning algorithm is said to be almost-surely asymptotically optimal if, as the number of samples approaches infinity, the probability of asymptotically converging to the optimum (Definition 2), if an optimal solution exists, is one,*

$$\mathbb{P}\left(\limsup_{n \rightarrow \infty} \min_{\pi \in \Sigma_n} \{c(\pi)\} = c^*\right) = 1, \quad (4)$$

where  $n$  is the number of samples,  $\Sigma_n \subset \Sigma$  is the set of all non-trivial paths found by the algorithm from those samples and  $c^*$  is the optimal solution cost.

## 2.2 Sampling-based motion planning

Sampling-based planning algorithms can be classified into multiple-query and single-query. Multiple-query planners construct a graph (roadmap), representing collision-free paths, that can be queried with multiple initial and goal states by computing the shortest path from initial to the goal state. On the other hand, single-query planners only focus on single initial and goal state pairs. The most commonly used algorithms are probabilistic roadmaps (PRMs; Kavraki et al. 1996; Hsu et al. 1998) for multiple-query and rapidly-exploring random trees (RRTs; LaValle and Kuffner Jr 2001) for single-query applications. These sampling-based planners are often effective in high-dimensional state spaces and save a large amount of computation by avoiding an explicit representation of obstacles in the state space as opposed to deterministic methods such as graph search-based planners. However, these planners only generate feasible solutions (collision-free paths), which may not be guaranteed to be optimal.

In Karaman and Frazzoli (2011), the authors propose new sampling-based multiple and single-query planners, PRM\* and RRT\*, the variants of PRMs and RRTs, which provide optimality guarantees. RRT\* works in a similar way to RRT by incrementally expanding a tree into the free

space, guided by randomly sampled states. However, unlike RRT, it takes into account nearby vertices surrounding this randomly sampled state to ensure that the most suitable parent vertex in the tree is selected. Moreover, RRT\* also considers the possibility of rewiring nearby vertices with respect to this randomly sampled state. This incremental rewiring process plays a crucial role in guiding RRT\* towards asymptotically converging to the optimal solution, a characteristic of paramount importance in sampling-based motion planning research.

The RRT# algorithm (Arslan and Tsiotras 2013) extends the exploitation process (local rewiring) of RRT\* to global rewiring by utilizing dynamic programming methods, resulting in an improvement of the speed of convergence rate. Removal of states that could not improve the current solution will help reduce the time required for convergence. In Karaman et al. (2011), the authors extend the RRT\* by introducing the online graph pruning algorithm called branch-and-bound. Here, a vertex in the current tree is deleted if the cost to reach this vertex, plus the lower-bound on the optimal cost to reach the goal (similar to A\* admissible heuristic) is more than the cost of the current solution path. These are the vertices that could not improve the current solution, and pruning them does help improve the RRT\* convergence time to enable efficient real-time operation. Moreover, modifications have been made to parent selection and rewiring processes of RRT\*. Instead of only considering a set of nearby vertices in a hypersphere as in RRT\*, Quick-RRT\* (Jeong et al. 2019) also considers their ancestry up to a user-defined parameter for possible parent candidates. A similar tree-extending algorithm is introduced in F-RRT\* (Liao et al. 2021), which creates random parent vertices near obstacles to find better initial solutions with a faster convergence rate.

Furthermore, various extensions have been proposed to accelerate the convergence rate such as bi-directional versions: RRT-Connect (Kuffner and LaValle 2000), RRT\*-Connect (Klemm et al. 2015), relaxing optimality to near-optimality: SPARS (Dobson and Bekris 2014), LBT-RRT (Salzman and Halperin 2016) and much more. Nevertheless, since the sampling process of these approaches employs uniform random distribution over the whole state space, the algorithm's convergence rate decreases as the number of dimensions increases, requiring longer computation time to generate optimal solutions.

## 2.3 State-space sampling

Prior work has been focused on increasing the efficiency of random sampling process of the sampling-based planning algorithms. In general, the performance of the planner highly depends on the distribution of random samples generated in each iteration. Many approaches rely on uniformly distributed samples over the whole state space to ensure that global optimality is preserved. However, the performance can often be improved by focusing the sampling on the regions with higher likelihood of finding better solutions.

In Bialkowski et al. (2013), the authors propose a biased-sampling technique which generates random samples from the approximated obstacle-free distribution space. They show that the distribution converges to a uniform distribution over the free space as the number of samples

approaches infinity. Similarly, Kim et al. (2014) decomposes the collision-free space into a set of spheres with varying radii called sampling cloud. Their Cloud RRT\* algorithm exploits this sampling cloud to generate random samples and constantly update it to refine the current best solution. In P-RRT\* and PQ-RRT\* algorithms (Qureshi and Ayaz 2016; Li et al. 2020), random samples are directionally guided by artificial potential fields (Khatib 1986) to efficiently explore the given environment. Unlike traditional rejection sampling approach (i.e., repeatedly sampling from the whole state space until a collision-free sample is found), these free-space biased sampling heuristic techniques quickly find better solutions and reduce the number of rejected samples however continue to sample the states that cannot improve the current solution.

Prior work has been focused on improving the random sampling process and the convergence rate of RRT\*. In Akgun and Stilman (2011), the authors proposed the bi-directional version of RRT\*, which uses path-biased sampling and heuristic sample rejection techniques to accelerate the planner convergence rate in high-dimensional planning problems. Similarly, these path biasing and path refinement ideas have been employed in Islam et al. (2012); Alterovitz et al. (2011) to improve the original RRT\* performance. However, these methods favor to find locally optimal solutions and decrease the likelihood of finding the samples that can improve the current solution. Moreover, techniques such as rectangular rejection sampling (Ferguson and Stentz 2006; Otte and Correll 2013) has also been applied to RRT\* to further improve the convergence rate and reduce the computational requirements. But, these approaches do not increase the probability of finding better solutions and their effectiveness decreases as the number of state dimensions grows.

To address these issues and accelerate the convergence of RRT\*, direct informed sampling technique is introduced in Gammell et al. (2014, 2018), which is demonstrated with Informed RRT\* algorithm. Informed RRT\* behaves the same as RRT\* until an initial solution is found. Once the initial solution is found, it biases the sampling on the subset of the state space (the  $L^2$  informed set), which is an  $n$ -dimensional hyperellipsoid with a traverse diameter of current solution cost. Unlike aforementioned techniques, this approach maintains the uniform sample distribution over the informed subset and considers all the states that could provide better solutions, and is still effective in higher dimensional state spaces. However, the solution path found by the planner may contain redundant states, leading to produce tortuous paths with many twists and turns, especially in the early phase of the planning process. This can, in fact, result in an unnecessary path cost with large informed sets, slowing down the convergence rate of the planner. Therefore, recent works have a great interest in integrating more advanced path refinement techniques with informed sampling to further reduce the size of the hyperellipsoid, thereby accelerating the convergence (Kim and Song 2015; Jiang et al. 2020; Wang et al. 2020b). Nevertheless, these advanced approaches can still be improved by incorporating greedy informed sampling heuristic (Section 3) to facilitate the exploitation process of the sampling-based planning algorithms.

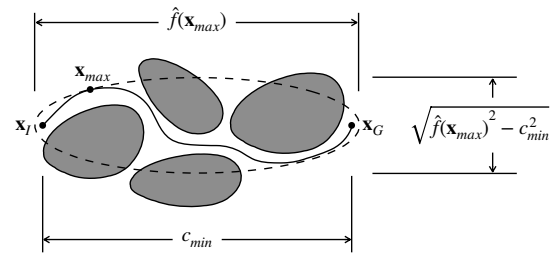


**Figure 3.** Illustration of the  $L^2$  greedy informed set,  $\mathcal{X}_{\hat{f}_{\text{greedy}}}$ , for an  $\mathbb{R}^2$  planning problem with path minimizing objectives. This greedy subset is highlighted in an ellipse with a dashed line and determined by the hypothetical minimum cost,  $c_{\min}$ , from an initial state,  $\mathbf{x}_I$ , to the goal state,  $\mathbf{x}_G$ , and the heuristics cost of a state in the solution path with highest admissible estimates,  $\hat{f}(\mathbf{x}_{\max})$ , as a transverse diameter.

Research has also shown interest in integrating bio-inspired methods (Wang et al. 2018, 2019), learning sampling heuristics (Wang et al. 2020a; Zhang et al. 2021; Wang et al. 2022) to effectively guide the tree growth towards the goal by restricting the sampling state space of the problem domain, achieving non-uniform sampling distribution.

### 3 Greedy Informed Set

Informed RRT\* has been proposed to improve the convergence rate of the RRT\* algorithm by utilizing direct informed sampling techniques, which performs sampling on the ellipsoidal subset of the planning domain, the  $L^2$  informed set (Definition 6). This informed subset is an estimate of the omniscient set (Definition 5), the set of states that can provide a better solution, and both sets provide the theoretical upper bounds on the probability of improving a solution in problems seeking to minimize path length in  $\mathbb{R}^n$ —see Gammell et al. (2018) for more details. However, since the informed set is an admissible estimate of the omniscient set and approximated based on the current path cost, not all randomly sampled states on the informed subset may be able to lead to an improvement of the current solution path. In other words, this may result in a larger ellipsoidal informed set with redundant samples, taking unnecessary computation time for converging to the optimal solution, especially in higher state dimensions. For instance, considering the planning problems with a large number of obstacles and tight spaces, the initial solution paths produced by the algorithm can be tortuous, with many twists and turns, resulting in a substantial informed set with a higher solution cost. Therefore, for the purpose of improving the algorithm’s convergence rate and reducing the size of the subset in these constrained scenarios with tortuous solution paths, this paper proposes a new direct informed sampling strategy, which does not rely on the cost of the current solution path. It only uses the maximum heuristic cost in the existing solution, which could be obtained by finding the heuristic value of the greedily chosen state in the current solution path. This new informed subset only accepts randomly sampled states that could guarantee better solution costs than the heuristic value of the greedily chosen state (Definition 7).

Once an initial solution is found by the planning algorithm, the set of states that can provide a better solution is formally defined as the *omniscient set* (Definition 5).

**Definition 5.** (Omniscient set). *Let  $g(\mathbf{x})$  be the cost-to-come of a state,  $\mathbf{x} \in \mathcal{X}$ , the true cost of the optimal path from the initial state  $\mathbf{x}_I$  to a state  $\mathbf{x}$  and  $h(\mathbf{x})$  be the cost-to-go of a state  $\mathbf{x}$ , the true cost of the optimal path from a state  $\mathbf{x}$  to the goal state  $\mathbf{x}_G$ ,*

$$\begin{aligned} g(\mathbf{x}) &= \min_{\pi \in \Sigma} \{c(\pi) \mid \pi(0) = \mathbf{x}_I, \pi(1) = \mathbf{x}\}, \\ h(\mathbf{x}) &= \min_{\pi \in \Sigma} \{c(\pi) \mid \pi(0) = \mathbf{x}, \pi(1) = \mathbf{x}_G\}. \end{aligned} \quad (5)$$

*Let  $f(\mathbf{x})$  be the true cost of the optimal path from the initial state  $\mathbf{x}_I$  to the goal state  $\mathbf{x}_G$ , constrained to pass through  $\mathbf{x}$ ,  $f(\mathbf{x}) = g(\mathbf{x}) + h(\mathbf{x})$ . We then define the omniscient set,  $\mathcal{X}_f$ , as the set of states in collision-free space,  $\mathcal{X}_{free}$ , that can provide better solutions than the current solution cost,  $c_i$ ,*

$$\mathcal{X}_f = \{\mathbf{x} \in \mathcal{X}_{free} \mid f(\mathbf{x}) < c_i\}. \quad (6)$$

Although sampling from this omniscient set is a necessary condition for RRT\*-like planners to improve the current solution, the exact knowledge of the set is unknown and requires solving the planning problem. Therefore, the estimates of the set are required to provide better solutions while maintaining the theoretical upper bounds (Definition 6).

**Definition 6.** ( $L^2$  Informed set). *Let the functions  $\hat{g}(\mathbf{x})$  and  $\hat{h}(\mathbf{x})$  be the  $L^2$  heuristic values of the cost-to-come of a state,  $\mathbf{x} \in \mathcal{X}$ , from the initial state,  $\mathbf{x}_I$ , and the cost-to-go from a state to the goal state,  $\mathbf{x}_G$ , respectively,*

$$\begin{aligned} \hat{g}(\mathbf{x}) &= \|\mathbf{x} - \mathbf{x}_I\|_2 \\ \hat{h}(\mathbf{x}) &= \|\mathbf{x}_G - \mathbf{x}\|_2 \end{aligned} \quad (7)$$

*where  $\|\cdot\|_2$  denotes the  $L^2$  norm (i.e., Euclidean distance) between two states. Let the function  $\hat{f}(\mathbf{x})$  be a  $L^2$  heuristic cost of a solution path from  $\mathbf{x}_I$  to  $\mathbf{x}_G$  constrained to pass through  $\mathbf{x}$ , i.e.,  $\hat{f}(\mathbf{x}) = \hat{g}(\mathbf{x}) + \hat{h}(\mathbf{x})$ . We then define the  $L^2$  informed set,  $\mathcal{X}_{\hat{f}}$ , as the set of states whose heuristic estimates can provide better solutions than the current solution cost,  $c_i$ ,*

$$\mathcal{X}_{\hat{f}} = \{\mathbf{x} \in \mathcal{X}_{free} \mid \hat{f}(\mathbf{x}) < c_i\}. \quad (8)$$

Moreover, this set is an upper bound estimate of the omniscient set and contains all the states that can yield better solutions, i.e.,  $\mathcal{X}_{\hat{f}} \supseteq \mathcal{X}_f$ , if its heuristic estimates never overestimate the path's true cost (*admissible heuristics*),

$$\forall \mathbf{x} \in \mathcal{X}, \hat{f}(\mathbf{x}) \leq f(\mathbf{x}). \quad (9)$$

Therefore, sampling or adding states from an admissible informed set is necessary to improve the current solution and maintain the uniform sample distribution over the sub-planning problem for the asymptotic optimality guarantees (Gammell et al. 2018).

However, in the case of complicated planning problems with many homotopy classes, the initial solution paths found by the planner may contain several twists and bends,

resulting in larger informed sets. This can, in fact, slow down the convergence rate of the planner, especially in high state dimensions, since the heuristic does not provide substantial information; or in other words there is a very low chance of drawing a random sample from the informed set that could also belong to the omniscient set. Hence, instead of relying on the existing solution cost to construct these large informed sets, the states that found the existing solution path can be utilized to build up the decreasing series of ellipses that are bounded from above by the admissible informed sets (Definition 7).

**Definition 7.** ( $L^2$  Greedy informed set). *Let  $\mathbf{x}_{max}$  be the state in the current solution path,  $\pi_i$ , with maximum admissible heuristics,*

$$\mathbf{x}_{max} := \arg \max_{\mathbf{x} \in \pi_i} \{\hat{f}(\mathbf{x})\}. \quad (10)$$

*We then define the  $L^2$  greedy informed set,  $\mathcal{X}_{\hat{f}_{greedy}}$ , as the set of all the states in obstacle-free space that could produce better solution costs than the heuristic cost of this greedily chosen state  $\mathbf{x}_{max}$  in the current solution (Figure 3),*

$$\mathcal{X}_{\hat{f}_{greedy}} = \{\mathbf{x} \in \mathcal{X}_{free} \mid \hat{f}(\mathbf{x}) < \hat{f}(\mathbf{x}_{max})\}. \quad (11)$$

Furthermore, it is bounded from above by the informed set, i.e.,  $\mathcal{X}_{\hat{f}_{greedy}} \supseteq \mathcal{X}_{\hat{f}}$  and will lead to smaller ellipsoidal regions compared to the original informed set, particularly in high-dimensional planning scenarios with complex solution paths. Consequently, sampling from this smaller subset will increase the likelihood of finding states that could belong to the omniscient set, thus facilitating faster convergence rates in improving the current solution path. However, because the greedy informed set is constructed based on the exploited knowledge of the existing solution path, similar to path biasing methods, it may or may not contain all the samples from the omniscient set, attempting to seek locally optimal solutions in certain planning contexts. Therefore, exploration into other homotopy classes, i.e., sampling from the informed set, remains essential for planners utilizing the greedy informed set to ensure global optimality and hold asymptotic optimality guarantees (see Section 4).

## 4 Greedy RRT\* (G-RRT\*)

Greedy RRT\* is an almost-surely asymptotically optimal path planning algorithm that build on top of RRT\*. Since it is a RRT\*-like algorithm, it rapidly explores the problem domain by building a tree through obstacle-free space with the help of random sampling. It also does the incremental rewiring of the growing tree to preserve the asymptotic optimality guarantees. However, instead of randomly sampling all over the problem domain throughout the entire planning process, G-RRT\* uses the direct informed sampling technique (Gammell et al. 2014, 2018) to focus the search only on the promising regions of the problem state space once the initial solution is found. Specifically, it uses a greedy version of informed set introduced in Section 3 to focus the search with the exploited knowledge of the existing solution path.

Finding the fast initial solution is important for G-RRT\* to make use of all the benefits of informed sets since RRT\*

and its informed versions behave the same before finding the initial solution. One way to accelerate the finding of initial solution is to leverage on bi-directional search, for example, bi-directional version of RRT (Kuffner and LaValle 2000) and its optimal variants (Klemm et al. 2015; Mashayekhi et al. 2020). Therefore, G-RRT\* improves the initial path finding time by leveraging on the concepts of bi-directional search. It maintains two rapidly growing trees, one rooted in the start and one in the goal, to explore the problem state space and uses a greedy connect heuristic to guide the tree towards each other similar to RRT-Connect (Kuffner and LaValle 2000).

---

**Algorithm 1: Greedy RRT\* ( $\mathbf{x}_I, \mathbf{x}_G$ )**


---

```

1  $V_a \leftarrow \{\mathbf{x}_I\}; E_a \leftarrow \emptyset; G_a = (V_a, E_a);$ 
2  $V_b \leftarrow \{\mathbf{x}_G\}; E_b \leftarrow \emptyset; G_b = (V_b, E_b);$ 
3  $E_{sol'n} \leftarrow \emptyset;$ 
4 for  $i = 1, \dots, n$  do
5    $c_i \leftarrow \text{ComputeBestCost}(E_{sol'n});$ 
6    $\mathbf{x}_{rand} \leftarrow \text{Sample}(\mathbf{x}_I, \mathbf{x}_G, c_i);$ 
7    $\text{status}, \mathbf{x}_a \leftarrow \text{Extend}^*(G_a = (V_a, E_a), \mathbf{x}_{rand});$ 
8   if  $\text{status} \neq \text{TRAPPED}$  then
9      $\text{status}, \mathbf{x}_b \leftarrow \text{Connect}^*(G_b = (V_b, E_b), \mathbf{x}_a);$ 
10    if  $\text{status} = \text{REACHED}$  then
11       $E_{sol'n} \leftarrow E_{sol'n} \cup \{\mathbf{x}_a, \mathbf{x}_b\};$ 
12     $\text{Swap}(G_a = (V_a, E_a), G_b = (V_b, E_b));$ 
13 return  $G = (V_a \cup V_b, E_a \cup E_b);$ 

```

---



---

**Algorithm 2: ComputeBestCost ( $E_{sol'n} = \{(v, w) \mid v \in V_a, w \in V_b\}$ )**


---

```

1  $c_i \leftarrow \infty;$ 
2  $\mathbf{x}_i \leftarrow \arg \min_{\mathbf{x} \in X_{sol'n}} \{g(\mathbf{x})\};$ 
3 if  $|X_{sol'n}| > 0$  then
4   if  $\epsilon > U([0, 1])$  then
5      $c_{max} \leftarrow -\infty;$ 
6      $\mathbf{x}_{best} \leftarrow \mathbf{x}_i;$ 
7     while  $\text{Parent}(\mathbf{x}_{best}) \neq \text{null}$  do
8        $c_{best} \leftarrow \hat{f}(\mathbf{x}_{best});$ 
9       if  $c_{best} > c_{max}$  then
10         $c_{max} \leftarrow c_{best};$ 
11         $\mathbf{x}_{best} \leftarrow \text{Parent}(\mathbf{x}_{best});$ 
12      $c_i \leftarrow c_{max};$ 
13   else
14      $c_i \leftarrow g(\mathbf{x}_i);$ 

```

---

#### 4.1 Notation

The state space of the path planning problem is denoted by  $\mathcal{X} \in \mathbb{R}^n$  where  $n \in \mathbb{N}$ . Those states that are in collision with obstacles are denoted by  $\mathcal{X}_{obs} \subseteq \mathcal{X}$  whereas valid collision-free states are denoted by  $\mathcal{X}_{free} = \mathcal{X} \setminus \mathcal{X}_{obs}$ . A notation  $\mathbf{x} \in \mathcal{X}$  represents a single state in the state space. The initial and goal states of the planning problem are denoted by  $\mathbf{x}_I \in \mathcal{X}_{free}$  and  $\mathbf{x}_G \in \mathcal{X}_{free}$  respectively.

A tree  $G = (V, E)$  is defined by a set of vertices  $V$  and edges  $E$ . The start tree is denoted by  $G_a = (V_a, E_a)$  and the

---

**Algorithm 3: Sample ( $\mathbf{x}_I, \mathbf{x}_G, c_{max}$ )**


---

```

1 repeat
2   if  $c_{max} < \infty$  then
3      $\mathbf{x}_{rand} \leftarrow$ 
4        $\text{SampleHyperEllipsoid}(\mathbf{x}_I, \mathbf{x}_G, c_{max});$ 
5     if  $\mathbf{x}_{rand} \in \mathcal{X} \cap \mathcal{X}_{PHS}$  then
6       return  $\mathbf{x}_{rand};$ 
7   else
8      $\mathbf{x}_{rand} \leftarrow \text{SampleUniform}(\mathcal{X});$ 
9     return  $\mathbf{x}_{rand};$ 
9 until  $\mathbf{x}_{rand}$  satisfies bounds;

```

---



---

**Algorithm 4: Extend\* ( $G = (V, E), \mathbf{x}$ )**


---

```

1  $\mathbf{x}_{nearest} \leftarrow \text{Nearest}(G = (V, E), \mathbf{x});$ 
2  $\mathbf{x}_{new} \leftarrow \text{Steer}(\mathbf{x}_{nearest}, \mathbf{x});$ 
3 if  $\text{ObstacleFree}(\mathbf{x}_{nearest}, \mathbf{x}_{new})$  then
4    $V \leftarrow V \cup \{\mathbf{x}_{new}\};$ 
5    $X_{near} \leftarrow \text{Near}(G = (V, E), \mathbf{x}_{new}, r_{rewire});$ 
6    $X_{ancestors} \leftarrow \text{Ancestors}(G = (V, E), X_{near}, r_{depth});$ 
7    $\mathbf{x}_{min} \leftarrow \mathbf{x}_{nearest};$ 
8   foreach  $\mathbf{x}_{near} \in (X_{near} \cup X_{ancestors})$  do
9      $c_{near} \leftarrow g(\mathbf{x}_{near}) + d(\mathbf{x}_{near}, \mathbf{x}_{new});$ 
10    if  $c_{near} < g(\mathbf{x}_{min}) + d(\mathbf{x}_{min}, \mathbf{x}_{new})$  then
11      if  $\text{ObstacleFree}(\mathbf{x}_{near}, \mathbf{x}_{new})$  then
12         $\mathbf{x}_{min} \leftarrow \mathbf{x}_{near};$ 
13     $E \leftarrow E \cup \{\mathbf{x}_{min}, \mathbf{x}_{new}\};$ 
14    foreach  $\mathbf{x}_{near} \in (X_{near} \cup X_{ancestors})$  do
15      if  $g(\mathbf{x}_{new}) + d(\mathbf{x}_{new}, \mathbf{x}_{near}) < g(\mathbf{x}_{near})$  then
16        if  $\text{ObstacleFree}(\mathbf{x}_{new}, \mathbf{x}_{near})$  then
17           $\mathbf{x}_{parent} \leftarrow \text{Parent}(\mathbf{x}_{near});$ 
18           $E \leftarrow E \setminus \{(\mathbf{x}_{parent}, \mathbf{x}_{near})\};$ 
19           $E \leftarrow E \cup \{(\mathbf{x}_{new}, \mathbf{x}_{near})\};$ 
20    if  $\mathbf{x}_{new} = \mathbf{x}$  then
21      return REACHED,  $\mathbf{x}_{new};$ 
22    else
23      return ADVANCED,  $\mathbf{x}_{new};$ 
24 return TRAPPED,  $\mathbf{x}_{new};$ 

```

---



---

**Algorithm 5: Connect\* ( $G = (V, E), \mathbf{x}$ )**


---

```

1 repeat
2    $\text{status}, \mathbf{x}_{new} \leftarrow \text{Extend}^*(G = (V, E), \mathbf{x});$ 
3 until  $\text{status} \neq \text{ADVANCED};$ 

```

---

goal tree is denoted by  $G_b = (V_b, E_b)$ . All the vertices in the start and goal trees  $V_a$  and  $V_b$  are directly associated with the valid regions of the state space  $\mathcal{X}_{free}$ . Edges in both trees  $E \subset V \times V$  are directed with a source vertex  $\mathbf{v}$  and a target vertex  $\mathbf{w}$ , represented by  $(\mathbf{v}, \mathbf{w})$ .

The cost of the connection from the source vertex  $\mathbf{v}$  to the target vertex  $\mathbf{w}$  in the graph  $G$  is denoted by the scalar  $c \in \mathbb{R}_{\geq 0}$  and its admissible heuristics is represented by  $\hat{c} \in \mathbb{R}_{\geq 0}$  where  $\forall v, w \in G, \hat{c}(\mathbf{v}, \mathbf{w}) \leq c(\mathbf{v}, \mathbf{w})$ . The true cost of the optimal path from the initial vertex to the specific vertex  $\mathbf{x}$ , also called, the cost-to-come of a vertex  $\mathbf{x}$ , is denoted by the function  $g(\mathbf{x}) = c(\mathbf{x}_I, \mathbf{x})$  and its admissible estimates by  $\hat{g}(\mathbf{x}) = \hat{c}(\mathbf{x}_I, \mathbf{x})$ . The true cost of the optimal path from

the vertex to the goal state, also called, the cost-to-go of a vertex is denoted by the function  $h(\mathbf{x}) = c(\mathbf{x}_I, \mathbf{x})$  and its admissible estimates by  $\hat{h}(\mathbf{x}) = \hat{c}(\mathbf{x}_I, \mathbf{x})$ .

The summation of these two heuristic estimates  $\hat{g}(\mathbf{x})$  and  $\hat{h}(\mathbf{x})$  defines the heuristic cost of the path from the start vertex  $\mathbf{x}_I$  passing through a specific vertex  $\mathbf{x}$  towards the goal vertex  $\mathbf{x}_G$ , i.e.,  $f(\mathbf{x}) = \hat{g}(\mathbf{x}) + \hat{h}(\mathbf{x})$ . This function  $f(\mathbf{x})$  also defines the informed set, i.e., the set of states whose heuristic estimates can provide better solutions than the current solution cost (Definition 6). The vertex with the maximum admissible heuristic cost in the path connected from the start vertex to the goal vertex is denoted by  $\mathbf{x}_{max}$ . This function  $f(\mathbf{x}_{max})$  defines the greedy informed set, i.e., the set of states whose heuristic estimates can provide better solutions than the heuristic cost of this greedily chosen state  $\mathbf{x}_{max}$  in the current solution (Definition 7).

## 4.2 Greedy Informed Sampling

G-RRT\* finds better solution paths to a planning problem by growing two trees,  $G_a = (V_a, E_a)$  from the start and  $G_b = (V_b, E_b)$  from the goal, consisting of the set of vertices,  $V_a \cup V_b$ , and edges,  $E_a \cup E_b$ , in free space towards randomly sampled states. These graphs are rewired with newly added vertices in such a way that the cost to come of the nearby vertices are minimized. Like Informed RRT\*, once an initial solution is found, it only focuses the random sampling on the subset of the problem domain with admissible ellipsoidal heuristics, thereby increasing the convergence rate towards the optimum. However, instead of exploring all the states within the informed subset that can improve the current solution cost, G-RRT\* differs from Informed RRT\* in that it exploits the current solution path information and biases the random sampling on the decreasing subset of the hyperellipsoid (the  $L^2$  greedy informed set). It also samples from the informed exploration subset to maintain the uniform sample distribution for asymptotic optimality guarantees. Specifically, G-RRT\* balances the exploration and exploitation of the random sampling process by introducing a parameter,  $\epsilon \in [0, 1]$ , called the *greedy biasing ratio*. If  $\epsilon = 0$ , it only focuses the sampling on the informed subset, behaving the same as Informed RRT\* algorithm with pure exploration. On the other hand, if  $\epsilon = 1$ , the algorithm exploits the current solution path information and only finds the set of states within the greedy informed set with no exploration. Therefore, a good balance between uniform sampling for exploration and path-biased sampling for exploitation is necessary to rapidly reduce the size of the informed subset for faster convergence rate and global optimality guarantees.

At each iteration, G-RRT\* finds the traverse diameter of the respective hyperellipsoids for random sampling process (Alg. 1, Line 5). First, it finds the current best goal vertex,  $\mathbf{x}_i$ , with the minimum cost-to-come value from the set of vertices in the goal region (Alg. 2, Line 2). With probability  $\epsilon$ , the algorithm determines the current maximum cost,  $c_i$ , for the sampling process by greedily selecting the best vertex in the existing solution path with maximum admissible heuristics (i.e., exploitation with  $L^2$  greedy informed set) (Alg. 2, Lines 4–12). With probability  $1 - \epsilon$ , it defines the current maximum cost by determining the cost required to

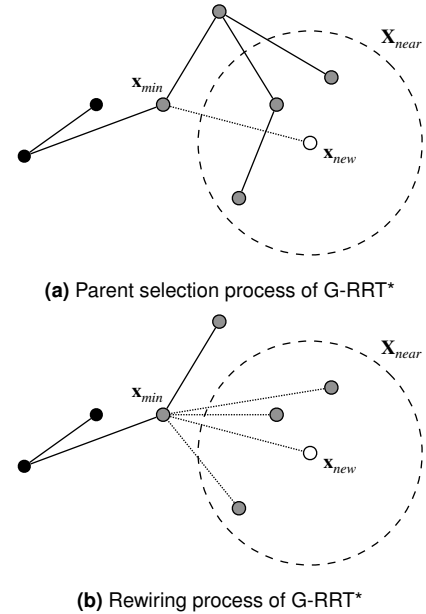


**Figure 4.** Incremental Q-RRT\*-style greedy parent selection and tree rewiring processes of G-RRT\* algorithm. The local neighbourhood of the newly added vertex  $\mathbf{x}_{new}$  is highlighted in circle with a dashed line while nearest vertices as well as their ancestors are denoted as gray dots. Black dots represent the rest of the vertices in the tree which does not include within a certain depth level.

reach the current best goal vertex (i.e., exploration with  $L^2$  informed set) (Alg. 2, Lines 13 and 14). The uniformly distributed random state can then be sampled from the hyperellipsoid if there exists a solution path (Alg. 1, Line 6, Alg. 3, Lines 2–5) or from the problem state space if no solution is found yet (Alg. 1, Line 6, Alg. 3, Lines 6–8).

## 4.3 Tree Extension

Once a new random sample has been found, G-RRT\* performs the tree extension process just as in RRT-Connect by connecting one tree towards the other and alternating between the two trees repeatedly. First, the selected tree is extended from the nearest vertex  $\mathbf{x}_{nearest}$  towards  $\mathbf{x}_{rand}$  using the Steer function also known as a local planner, resulting in  $\mathbf{x}_{new}$  (Alg. 1, Line 7, Alg. 4, Lines 1–2). If the resulting edge from the nearest vertex  $\mathbf{x}_{nearest}$  to the new vertex  $\mathbf{x}_{new}$  is valid,  $\mathbf{x}_{new}$  is added to the set of vertices  $V$  of the current tree (Alg. 1, Line 7, Alg. 4, Lines 3–4). To achieve almost-sure asymptotic optimality, G-RRT\* does the incremental tree rewiring techniques in the local neighbourhood of the newly added vertex  $\mathbf{x}_{new}$  as in RRT\*. However, G-RRT\* also considers outside of the neighbour hood, i.e., it takes into consideration of the ancestors of  $X_{near}$  up to a certain depth level similar to Q-RRT\* algorithm. This parent selection process tends to result in more straighten tree edges with lower cost initial solutions compared to only using the nearby vertices  $X_{near}$ . Similarly, these ancestors are also considered during the tree rewiring procedure to check whether they can improve any of  $\mathbf{x}_{new}$ 's neighbours. Figure 4 illustrates the greedy parent selection and rewiring processes of the G-RRT\* algorithm.

**Definition 8.** (Predecessor of a vertex). Let  $\mathbf{v}$  be a vertex in a tree  $G = (V, E)$  defined by a set of vertices  $V$  and edges  $E$ . We then define the predecessor of  $\mathbf{v}$ , denoted by  $\text{pred}(\mathbf{v}) = \mathbf{u}$ , as a parent vertex of  $\mathbf{v}$  which has a directed edge leading into  $\mathbf{v}$  in  $G$  where  $\mathbf{u}, \mathbf{v} \in V$  and  $(\mathbf{u}, \mathbf{v}) \in E$ .

**Definition 9.** (Ancestor of a vertex). Let  $\mathbf{v}$  be a vertex in a tree  $G = (V, E)$  defined by a set of vertices  $V$  and edges  $E$ . Let  $d$  be the depth level above  $\mathbf{v}$  in the tree. We then define the ancestor of a vertex at  $d$ -th parent as the vertex that is  $d$  levels above  $\mathbf{v}$  in the tree, following the path towards the root start vertex  $\mathbf{x}_I$ :

$$\text{ancestor}_d(\mathbf{v}) = \text{pred}^{(d)}(\mathbf{v}) \quad (12)$$

where  $\text{pred}^{(d)}(\mathbf{v})$  represents recursively applying the predecessor function  $d$  times starting from vertex  $\mathbf{v}$ .

**Definition 10.** (Ancestry set). Let  $S$  be the set of vertices in a tree  $G = (V, E)$  defined by a set of vertices  $V$  and edges  $E$ . We define the ancestry set of  $S$ , denoted by  $X_{\text{ancestors}}(S)$ , as the set containing all vertices that are ancestors of any vertex in  $S$  up to the  $d$ -th parent. Formally, for  $d \geq 1$ , the ancestry set is given by:

$$X_{\text{ancestors}}(S) = \bigcup_{\mathbf{v} \in S} \bigcup_{i=1}^d \text{ancestor}_i(\mathbf{v}) \quad (13)$$

Once a new vertex  $\mathbf{x}_{\text{new}}$  is added into the tree, G-RRT\* finds the best potential parent vertex for this newly added state by considering the cost-to-come to a set of nearby vertices defined by the local neighborhood radius (Alg. 1, Line 7, Alg. 4, Line 5). It also considers the ancestry set  $X_{\text{ancestors}}$  of  $X_{\text{near}}$  (Definition 10) up to a certain depth level during this parent selection process (Alg. 1, Line 7, Alg. 4, Line 6). If connecting to a vertex from these candidate parent sets improves the current cost-to-come to a newly added vertex  $\mathbf{x}_{\text{new}}$  and the edge is valid, this resulting edge from the best parent vertex  $\mathbf{x}_{\text{min}}$  to  $\mathbf{x}_{\text{new}}$  is added to a set of edges  $E$  of the current tree (Alg. 1, Line 7, Alg. 4, Lines 7–13).

G-RRT\* also considers this ancestry set  $X_{\text{ancestors}}$  during its rewiring process. If connecting to either a new vertex  $\mathbf{x}_{\text{new}}$  or one of the ancestors can lower the cost-to-come of the nearby vertices, they are rewired to be the descendants of this vertex if the new edge is collision-free (Alg. 1, Line 7, Alg. 4, Lines 14–19). Similar to RRT-Connect algorithm, tree extension process of G-RRT\* also results in three output states: REACHED if a newly generated vertex  $\mathbf{x}_{\text{new}}$  reaches an input vertex  $\mathbf{x}$  (Alg. 1, Line 7, Alg. 4, Lines 20–21), ADVANCED if  $\mathbf{x}_{\text{new}} \neq \mathbf{x}$  is added to the vertex set (Alg. 1, Line 7, Alg. 4, Lines 22–23) and TRAPPED if the edge from  $\mathbf{x}_{\text{nearest}}$  to  $\mathbf{x}_{\text{new}}$  is in collision (Alg. 1, Line 7, Alg. 4, Line 24).

#### 4.4 Greedy Connect Heuristic

Certain planning problems are extremely challenging for planners to find the paths especially when either start or goal states (or both) are blocked by enclosures or narrow passages (for example, problems in Figures 6b and 6c). This difficulty increases as the state dimension grows, making RRTs impractical to be used in higher state space applications. In our work, we tackle this problem by relying on a bi-directional search, maintaining two separate RRT

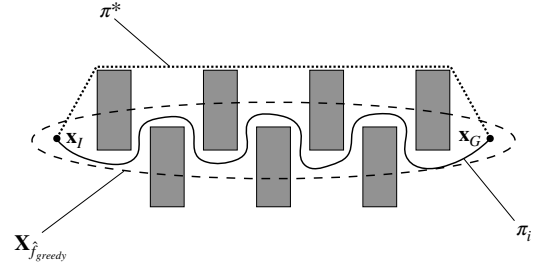


**Figure 5.** Illustration of the sub-optimality of greedy informed set in an example planning scenario. The  $L^2$  greedy informed set,  $X_{f_{\text{greedy}}}$ , highlighted in a dashed ellipse, is constructed based on the current tortuous solution path,  $\pi_i$ . The true optimal path,  $\pi^*$ , is depicted as a dotted line. Here, the greedy informed set does not contain all the vertices that can improve the current solution cost (i.e., those that contribute to approaching  $\pi^*$  and lie outside of the hyperellipsoid) due to the nature of its greedy exploitation.

trees at the start and goal states respectively. In each iteration, while one tree is extended toward the randomly generated state using the EXTEND\* procedure (Section 4.3), G-RRT\* attempts to connect the newly added vertex to the nearby vertex of the other tree using the greedy CONNECT heuristic similar to RRT-Connect algorithm. It then alternates between the steps by swapping the two trees. This approach helps G-RRT\* to find paths quickly in these challenging situations by using the benefits of uniform explorative nature of RRTs to avoid the local minima pitfalls while exploiting with greedy connection strategy to connect the two trees.

Once a tree extension process towards the randomly generated vertex is succeeded, G-RRT\* attempts to extend the other tree towards the newly added vertex of the current tree using the greedy CONNECT\* heuristic (Alg. 1, Lines 8–9). This process iteratively calls EXTEND\* until the other tree either reaches a newly added vertex or fails to do the extension anymore due to the collision in edge (Alg. 5). If this connection is succeeded, i.e., the other tree successfully connects the newly added vertex of the current tree, solution path is found and this edge is added to the solution edge set  $E_{\text{sol'n}}$  which maintains all the edges connecting the two trees (Alg. 1, Lines 10–11). In order to make sure both trees are growing towards each other greedily, G-RRT\* swaps the two trees before proceeding the next iteration of the algorithm (Alg. 1, Line 12).

## 5 Analysis

### 5.1 Probabilistic completeness

A path planning algorithm is considered *robustly feasible* if there exists a solution path with strong  $\delta$ -clearance (i.e., a distance  $\delta$  away from any obstacle in  $\mathcal{X} \in \mathbb{R}^n$ ) for some  $\delta > 0$  (Karaman and Frazzoli 2011). An algorithm for solving any robustly feasible planning problem  $(\mathcal{X}_{\text{free}}, \mathbf{x}_I, \mathbf{x}_G)$  has *probabilistic completeness* guarantees if there exists a goal vertex  $\mathbf{x}_G$  in the graph where a start vertex  $\mathbf{x}_I$  becomes connected to  $\mathbf{x}_G$  as the number of samples approaches infinity (Definition 3). In other words, the algorithm is said to be probabilistically complete, if given sufficient time, it can find a solution to the path planning problem if one exists.

G-RRT\* maintains two rapidly growing trees, each of which fulfills the probabilistic completeness property of classical RRTs. This means that during the alternating extension process of each RRT tree, new vertices are added to the sets  $V_a$  and  $V_b$  of start and goal trees where  $V_k = V_a \cup V_b$  approaches  $\mathcal{X}$  in probability with  $V_k$  being the set of RRT vertices after iteration  $k$ . Since the greedy CONNECT heuristic generates all the typical RRT vertices along with additional ones, it aids in covering  $\mathcal{X}_{\text{free}}$ , and therefore does not adversely affect the convergence results.

## 5.2 Asymptotic optimality

Consider a robustly feasible path planning problem defined by the state space  $\mathcal{X}_{\text{free}}$ , initial state  $\mathbf{x}_I$ , and goal state  $\mathbf{x}_G$ , we define the optimal path planning problem as to find a path  $\pi^*$  from  $\mathbf{x}_I$  to  $\mathbf{x}_G$  that minimizes a cost function  $c: \Sigma \rightarrow \mathbb{R}_0^+$  where  $\Sigma$  is the set of all feasible paths (Definition 2). A solution path  $\pi^*$  is considered robustly optimal if there exists another path  $\pi_0$  with strong  $\delta$ -clearance in the same homotopy class where  $c(\pi_0) = \min\{c(\pi) : \pi \text{ is feasible}\}$  (Karaman and Frazzoli 2011). A solution path  $\pi^*$  is considered *asymptotically optimal* if, for any robustly feasible planning problem ( $\mathcal{X}_{\text{free}}, \mathbf{x}_I, \mathbf{x}_G$ ) and cost function  $c: \Sigma \rightarrow \mathbb{R}_0^+$  that produces a robustly optimal solution, the following holds:

$$P(\limsup_{n \rightarrow \infty} Y_n = c^*) = 1 \quad (14)$$

where  $Y_n \geq c^*, \forall n \in \mathbb{N}$  is the cost of the best solution found in the graph  $G$  at the end of iteration  $n$  and  $c^*$  is the theoretical minimum cost (Definition 4).

RRT\* has proven to be asymptotically optimal by incrementally rewiring the tree around new vertices (Karaman and Frazzoli 2011). These are the set of vertices which are within the  $n$ -dimensional unit ball of radius,  $r_{\text{rewire}}$ , of the newly added vertex in the Euclidean space:

$$r_{\text{rewire}} = \min\{\eta, r_{\text{RRT}^*}\} \quad (15)$$

where  $\eta > 1$  represents the maximum adjustable edge length of the tree, while  $r_{\text{RRT}^*}$  is a function that depends on the problem measure and the number of vertices in the current tree. Here,

$$r_{\text{RRT}^*} := \left( 2 \left( 1 + \frac{1}{n} \right) \left( \frac{\lambda(\mathcal{X}_{\text{free}})}{\zeta_n} \right) \left( \frac{\log(|V|)}{|V|} \right) \right)^{\frac{1}{n}} \quad (16)$$

where  $\lambda(\cdot)$  denotes the Lebesgue measure of a set,  $\zeta_n$  represents the Lebesgue measure of an  $n$ -dimensional unit ball,  $|\cdot|$  indicates the cardinality of a set, with  $n$  denoting the number of dimensions in the state space.

Direct informed sampling approaches have also shown to be maintaining the property of asymptotic optimality of RRT\* however they only search on a subset of the original planning problem (Gammell et al. 2014, 2018). Therefore, this reduces the computational requirements of rewiring at each planning iteration due to the smaller number of rewiring neighborhoods. Here, the rewiring requirements to maintain the asymptotic optimality in the smaller subset of the planning domain is a function of the number of vertices in the informed set,  $|V \cap \mathcal{X}_{\hat{f}}|$ , and its measure,  $\lambda(\mathcal{X}_{\hat{f}})$ .

G-RRT\* uses the greedy informed set  $\mathcal{X}_{\hat{f}_{\text{greedy}}}$  described in Section 3 to focus the search on even smaller subset of the planning domain than the informed set, where, it is bounded from above by the informed subset, i.e.,  $\mathcal{X}_{\hat{f}_{\text{greedy}}} \supseteq \mathcal{X}_{\hat{f}}$ . This increases the chances of finding the vertices that are more likely to be inside the omniscient set (Definition 5), improving the rate of converging to the optimal solution. Here, the rewiring requirements of G-RRT\* is a function of the number of vertices in the greedy informed set,  $|V \cap \mathcal{X}_{\hat{f}_{\text{greedy}}}|$ , and its measure,  $\lambda(\mathcal{X}_{\hat{f}_{\text{greedy}}})$  where

$$r_{\text{G-RRT}^*} := \left( 2 \left( 1 + \frac{1}{n} \right) \left( \frac{\lambda(\mathcal{X}_{\hat{f}_{\text{greedy}}})}{\zeta_n} \right) \left( \frac{\log(|V \cap \mathcal{X}_{\hat{f}_{\text{greedy}}}|)}{|V \cap \mathcal{X}_{\hat{f}_{\text{greedy}}}|} \right) \right)^{\frac{1}{n}} \quad (17)$$

However, not all vertices in the greedy informed set is guaranteed to be in the omniscient set since it is an overly approximated version of it which may or may not be an upper bound estimate of the true omniscient set (see Figure 5). In other words, vertices that can lead to better solution paths may exist in outside homotopy regions of the greedy informed set. Since G-RRT\* also samples from the informed subset based on the greedy biasing ratio (See Section 4.2), it still holds the asymptotic optimality guarantees of direct informed sampling techniques.

## 6 Simulation and Experiments

Greedy RRT\* was compared against the Open Motion Planning Library (OMPL; Sucan et al. 2012) implementations of RRT-Connect, RRT\*, Informed RRT\*, RRT\*-Connect (Klemm et al. 2015), BIT\* (Gammell et al. 2020) and AIT\* (Strub and Gammell 2020, 2022) on simulated planning problems in  $\mathbb{R}^2$ ,  $\mathbb{R}^4$ ,  $\mathbb{R}^8$  and  $\mathbb{R}^{16}$  (Section 6.1), manipulation problems for two Barret WAM arms with 14 degrees-of-freedom ( $\mathbb{R}^{14}$ ) in the Open Robotics Automation Virtual Environment (OpenRAVE; Diankov 2010) (Section 6.2) and real-world planning problem for a self-reconfigurable mobile robot Panthera in SE(2) and SE(2) +  $\mathbb{R}^2$  state spaces (Section 6.3)\*. Planner developer tools (PDT; Gammell et al. 2022) was used to run all the experiments.

The planners were tested with the optimization objective of minimizing path length. All the planners used maximum edge lengths of 0.3, 0.4, 0.5, 0.65, 1.25, 2.4 and 3.0 in  $\mathbb{R}^2$ , SE(2),  $\mathbb{R}^4$ , SE(2) +  $\mathbb{R}^2$ ,  $\mathbb{R}^8$ ,  $\mathbb{R}^{14}$  and  $\mathbb{R}^{16}$  respectively. An RGG constant of  $\eta = 1.001$  was used for all the planners and the Euclidean distance (i.e.,  $L^2$  norm) for path length was used as admissible cost heuristics. BIT\*-based planners used a batch size of 100 and G-RRT\* used the greedy biasing ratio of  $\epsilon = 0.9$  to urge the exploitation in all the experiments.

### 6.1 Abstract planning problems

The planners were tested on three simulated planning problems in  $\mathbb{R}^2$ ,  $\mathbb{R}^4$ ,  $\mathbb{R}^8$ , and  $\mathbb{R}^{16}$  as depicted in Figure 6.

\*Simulations were run in Ubuntu 22.04 docker on a MacBook Air with 16 GB of RAM and Apple M2 chip.

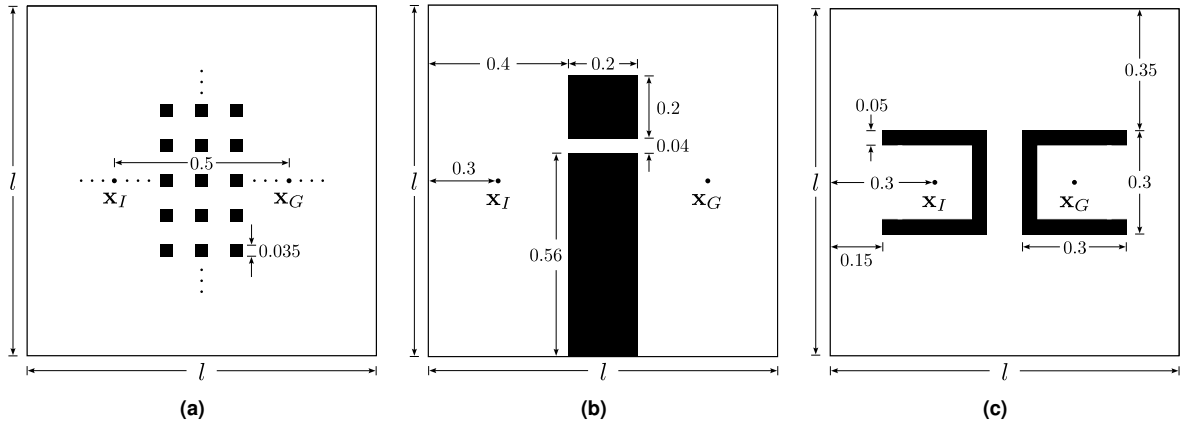


**Figure 6.** Illustrations of the simulation experiments on which the planners were tested. These include complex planning problems containing (a) many homotopy classes, (b) narrow passage gap environment and (c) double enclosures with a problem domain of size  $l = 1$ . The  $x_I$  and  $x_G$  represent the initial and goal states respectively.

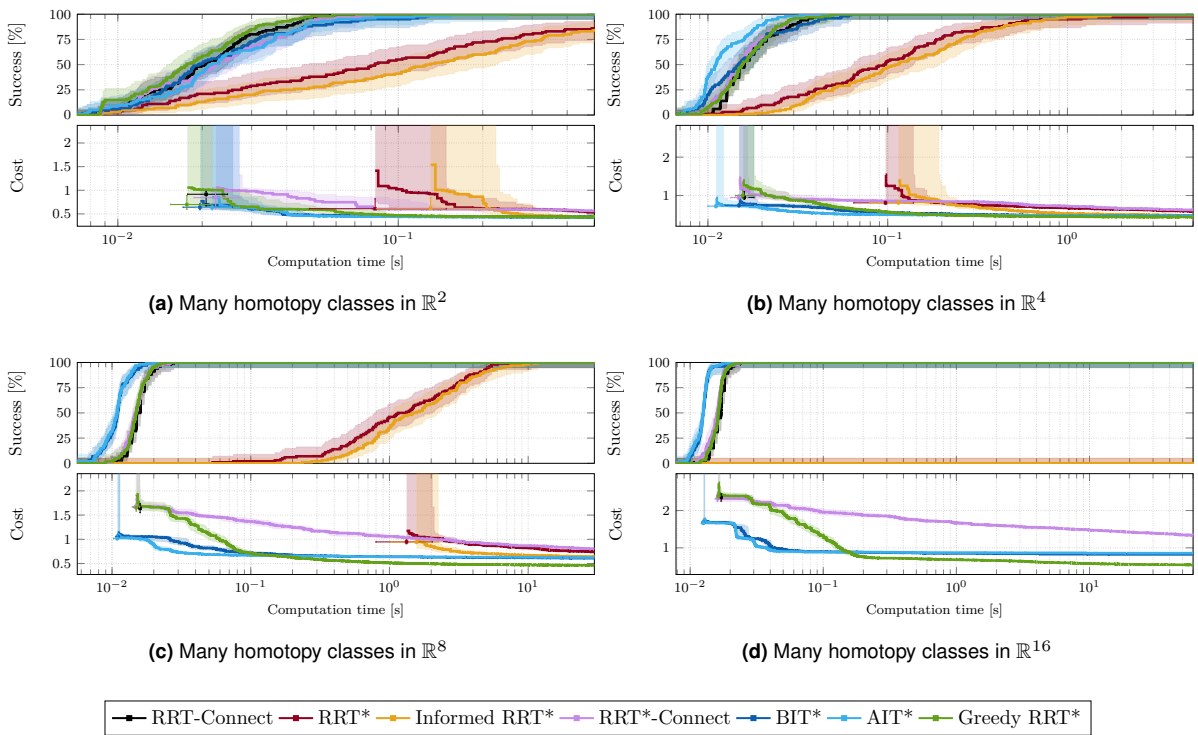


**Figure 7.** Planner performances versus running time on the many homotopy classes problem described in Section 6.1 (Figure 6a). The success plots represent the percentage of number of successful runs over time and the cost plots show the median solution cost versus run time for each planner. The error bars and shaded areas denote non-parametric 99% confidence intervals on the median. Each planner was run for 100 trials with running times of 0.5, 5.0, 30.0 and 100.0 seconds in  $\mathbb{R}^2$ ,  $\mathbb{R}^4$ ,  $\mathbb{R}^8$  and  $\mathbb{R}^{16}$ , presented in plots (a), (b), (c) and (d), respectively.

The first problem consists of many axis-aligned homotopy classes and/or (hyper)rectangles, filled over the whole problem state space, where the initial and goal states are located at  $[-0.25, 0.0, \dots, 0.0]^T$  and  $[0.25, 0.0, \dots, 0.0]^T$ , respectively (Figure 6a). The second problem contains two homotopy classes with a narrow passage gap of width 0.04, where the initial and goal states are located at  $[-0.3, 0.0, \dots, 0.0]^T$  and  $[0.3, 0.0, \dots, 0.0]^T$ , respectively (Figure 6b). The last experiment is a challenging dual-enclosure problem from planning literature, consisting of two hollow axis-aligned (hyper)rectangles enclosing the initial and goal states. Here, the initial and goal states are located at  $[-0.3, 0, \dots, 0]^T$  and  $[0.3, 0, \dots, 0]^T$ , respectively

(Figure 6c). Note that, the planning time given to the planners varies based on the difficulty of the problem domain and the number of state dimensions. Each planner was run 100 trials with different pseudorandom seeds in which the solution cost was recorded every  $10^{-4}$  seconds by a separate thread. If the solution is not found yet during recording, we set the value of a solution cost to be infinity for the purpose of calculating the median. Figures 7, 8 and 9 present the performance of the tested planners on these planning problems, where the median solution cost of each planner, together with its success rate is plotted versus computation time.

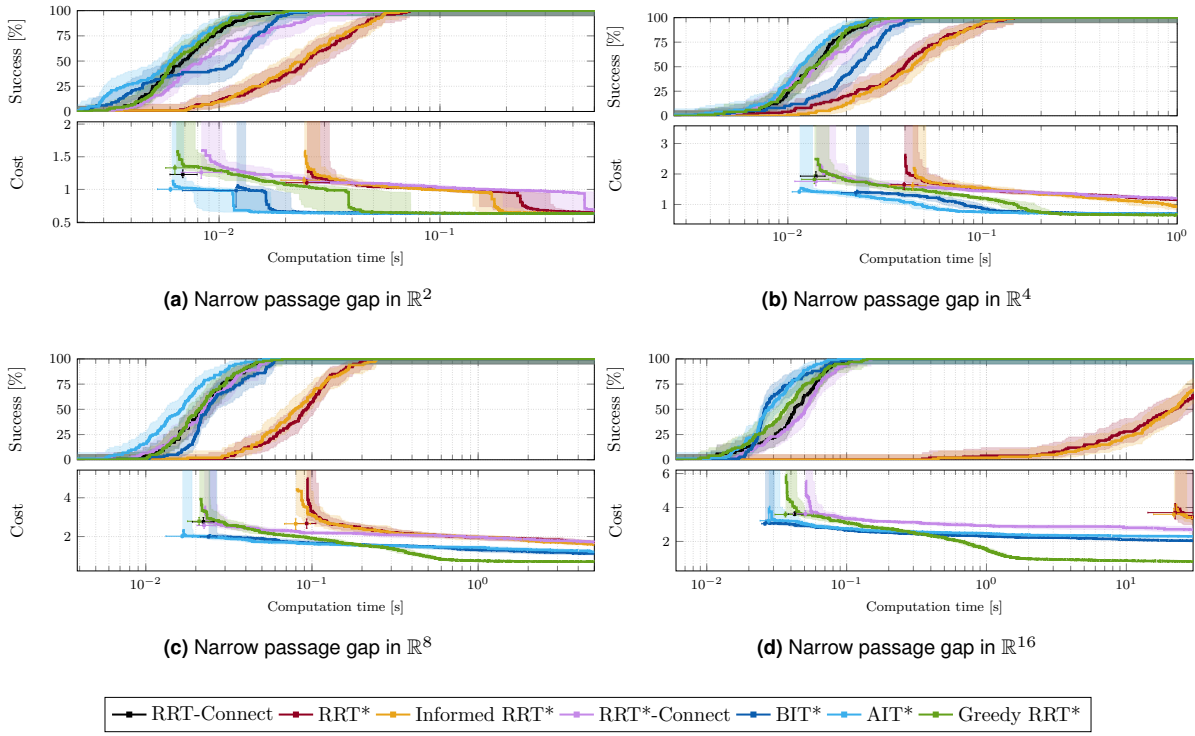


**Figure 8.** Planner performances versus running time on the narrow passage gap problem described in Section 6.1 (Figure 6b). The success plots represent the percentage of number of successful runs over time and the cost plots show the median solution cost versus run time for each planner. The error bars and shaded areas denote non-parametric 99% confidence intervals on the median. Each planner was run for 100 trials with running times of 0.5, 1.0, 5.0 and 30.0 seconds in  $\mathbb{R}^2$ ,  $\mathbb{R}^4$ ,  $\mathbb{R}^8$  and  $\mathbb{R}^{16}$ , presented in plots (a), (b), (c) and (d), respectively.

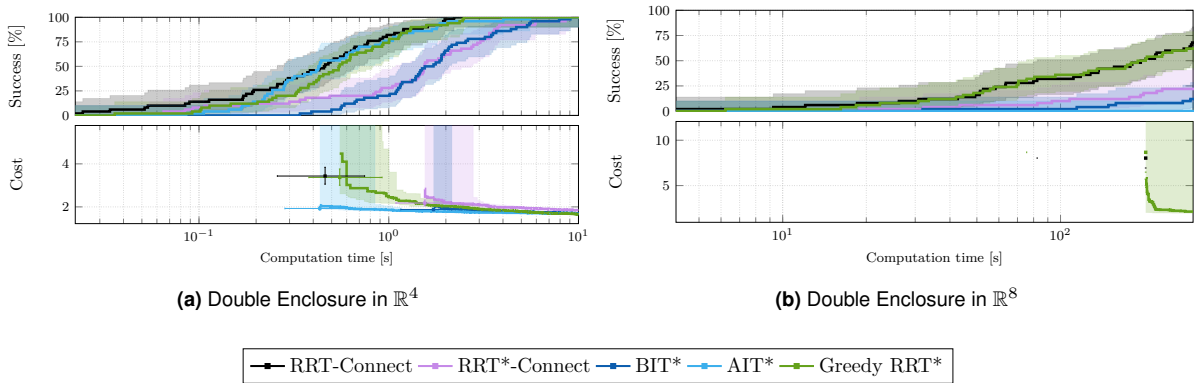


**Figure 9.** Planner performances versus running time on the double enclosure problem described in Section 6.1 (Figure 6c). The success plots represent the percentage of number of successful runs over time and the cost plots show the median solution cost versus run time for each planner. The error bars and shaded areas denote non-parametric 99% confidence intervals on the median. Each planner was run for 50 trials with running times of 10.0 and 300.0 seconds in  $\mathbb{R}^4$  and  $\mathbb{R}^8$ , presented in plots (a) and (b), respectively.

These results demonstrate the necessity of exploitation techniques in sampling-based planners for tackling challenging planning problems. G-RRT\* performs comparably to AIT\* and BIT\* in lower state dimensions and consistently outperforms all other RRT\*-based algorithms. It finds solutions in every trial with a 100% success rate and is competitive with RRT-Connect algorithm in terms of success rate. In higher dimensions, G-RRT\* outperforms all the anytime sampling-based planners, especially in converging to the optimal solutions.

From the results, we can observe that the performance of the RRT-based planners decreases as the state dimension grows. These single-tree planners struggle to find solutions

within the available planning time, especially in  $\mathbb{R}^{16}$  for the experiments from Figures 6a and 6b. Note that we omitted running single-tree RRT versions in the double enclosures experiment (Figure 6c) since it is a highly challenging problem, widely recognized as a *bug trap* problem, for any sampling-based planning algorithm in high dimensions (Yershova et al. 2005).

**6.1.1 Problems with axis-aligned homotopy classes** In this problem involving many axis-aligned homotopy classes (Figure 6a), there is not much difference in performance between the planners in  $\mathbb{R}^2$  and  $\mathbb{R}^4$  (Figures 7a and 7b). Here, G-RRT\*, BIT\*, AIT\*, and RRT-Connect find solutions faster

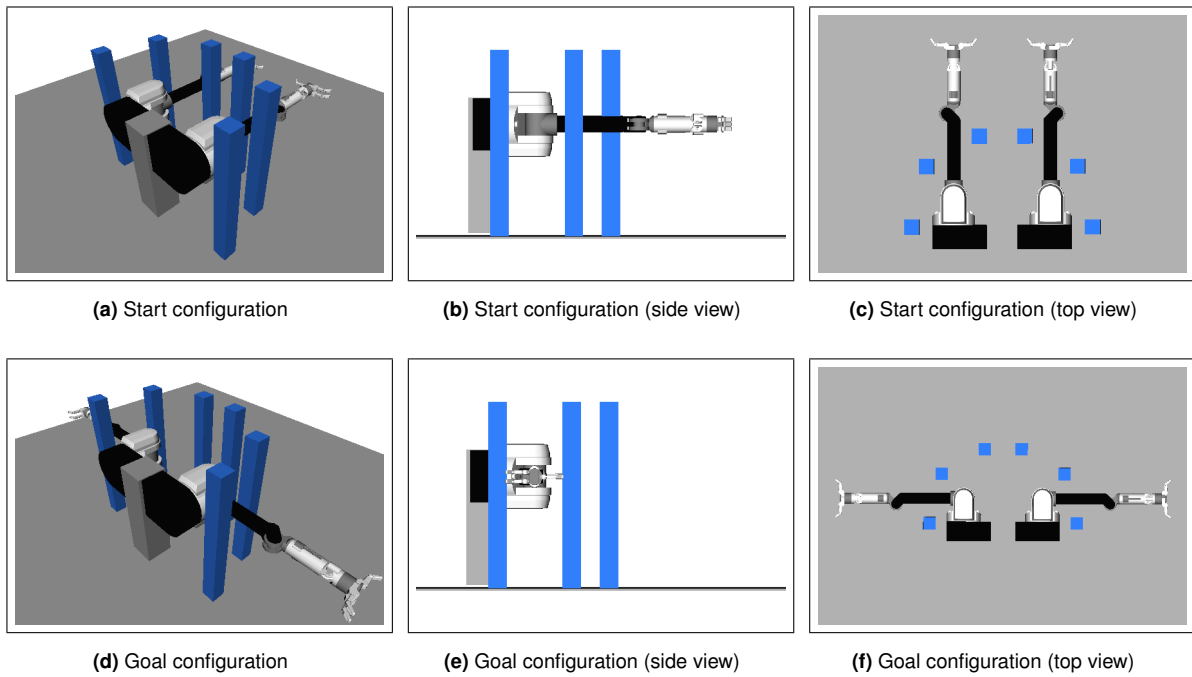


**Figure 10.** A dual-arm manipulation problem for the Barrett WAM Arm in  $\mathbb{R}^{14}$ . Starting from the configuration of the arms pointing in the same direction (a-c), the arms must be moved to extend outward in opposite directions without hitting the cage (d-f).

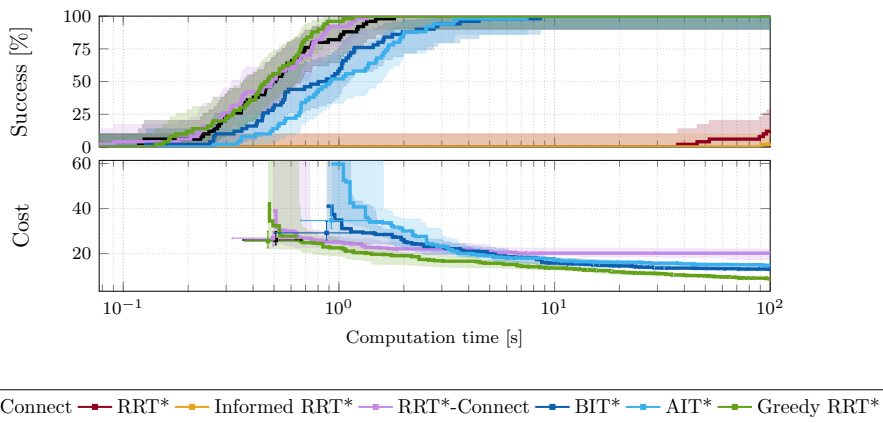


**Figure 11.** Planner performances versus running time on the manipulation experiment described in Section 6.2 (Figure 10). The success plots represent the percentage of a number of successful runs over time and the cost plots show the median solution cost versus run time for each planner. The error bars and shaded areas denote non-parametric 99% confidence intervals on the median. Each planner was run for 50 trials with running time of 100.0 seconds in  $\mathbb{R}^{14}$ .

than other RRT\*-based planners with a similar success rate. However, as the state dimension grows—i.e., in  $\mathbb{R}^8$  and  $\mathbb{R}^{16}$ , G-RRT\* outperforms all the tested planners in converging to the lowest cost in a shorter time period, followed by BIT\* and AIT\* algorithms (Figures 7c and 7d). Note that in  $\mathbb{R}^{16}$  problems, RRT\*-based planners are not able to find solutions within the available time budget.

**6.1.2 Narrow passage gap problems** In this experiment involving a narrow passage gap (Figure 6b), all the tested planners were able to find solutions in  $\mathbb{R}^2$  and  $\mathbb{R}^4$  problems with a 100% success rate (Figures 8a and 8b). Here, G-RRT\*, BIT\*, and AIT\* planners converge to the optimum at a similar rate when finding a solution through a narrow passage gap. However, RRT\*-based algorithms struggle to find a path through the narrow passage gap in  $\mathbb{R}^4$ . On the other hand, there is a noticeable performance change in higher state dimensions, such as  $\mathbb{R}^8$  and  $\mathbb{R}^{16}$  problems.

All asymptotically optimal planners struggle to find a path through a narrow passage gap, but G-RRT\* is the only planner that is able to find a path through it within the available time budget, and the difference becomes larger as the state dimension increases (Figures 8c and 8d).

**6.1.3 Double enclosures problems** We also conducted experiments on challenging problems involving double enclosures symmetric around the start and goal states. Since all asymptotically optimal sampling-based planners struggled to solve this problem as state dimensions increased, it was only run for  $\mathbb{R}^4$  and  $\mathbb{R}^8$  problems, and RRT\*-based planners were omitted from the experiments. In  $\mathbb{R}^4$ , all the tested planners were able to solve the problem within the available time and showed comparable performance in converging to the optimum (Figure 9a). However, all asymptotically optimal planners struggled to solve this

problem in higher state dimensions, specifically in  $\mathbb{R}^8$ . G-RRT\* and RRT-Connect were the only planners that found a solution in more than 50% of the trials (Figure 9b). This demonstrates the importance of maintaining two greedily connecting trees in problems involving several biased Voronoi regions (Yershova et al. 2005). Nevertheless, since RRT-Connect is a non-anytime planner that cannot converge to the optimum, G-RRT\* is the only almost-surely asymptotically optimal planner that requires less time to find better median solution costs within an available planning time in higher state dimensions.

## 6.2 Manipulation Problems

The planners were also tested on manipulation tasks involving Barrett Whole-Arm Manipulator (WAM) arms within the Open Robotics Automation Virtual Environment (OpenRAVE; Diankov 2010). OpenRAVE was set up to utilize the Flexible Collision Library (FCL; Pan et al. 2012), with a collision checking resolution set at  $10^{-2}$ . Figure 10 depicts the dual-arm planning experiment for two Barrett WAM arms with 14 degrees-of-freedom. The objective is to move them from an initial configuration, where they point in the same forward direction, to a goal configuration where the arms are extended outward in opposite directions without colliding with the cage. Results for the performance of all the tested algorithms when optimizing path length are illustrated in Figure 11.

From the results, it is evident that RRT\* and Informed RRT\* planners struggle to find solutions within the available planning time due to the high dimensionality of state spaces. In contrast, G-RRT\* quickly finds initial solutions, as fast as RRT-Connect and RRT\*-Connect algorithms, all achieving a 100% success rate, followed by BIT\* and AIT\* planners. In summary, G-RRT\* outperforms all tested asymptotically optimal planners in converging to optimal solutions, while also matching the speed of non-optimal planners in finding initial solutions.

## 6.3 Planning for Panthera reconfigurable robot in real-world environment

We validate the proposed G-RRT\* algorithm with a self-reconfigurable robot, Panthera, developed by Hayat et al. (2019) as a case study. Panthera has four independent steering units designed for omnidirectional locomotion. Its body frame can also be expanded and compressed by independently controlling the additional two gaits to traverse tight spaces, as observed in Figure 12. The state of Panthera in the world frame can then be represented as a 5-dimensional space,  $x, y, \theta, j_0, j_1$ , where  $x, y, \theta$  denotes the SE(2) state space, and  $j_0, j_1$  are the two controllable gaits of Panthera in  $\mathbb{R}^2$ . Here, the angles for each steering unit of Panthera are not considered during planning since this paper focuses only on geometric path planning. The resultant paths from the planners consist solely of waypoints representing the robot's state space, and an external local trajectory controller is responsible for following these generated waypoints.

To evaluate the efficiency of saving energy and time of different trajectories generated from a predefined source to destination inside the real-world environment, the

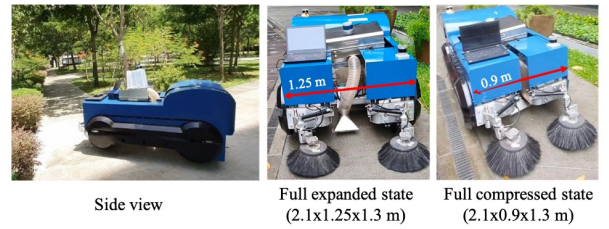


**Figure 12.** Panthera reconfigurable pavement sweeping platform with expanded and compressed ability.

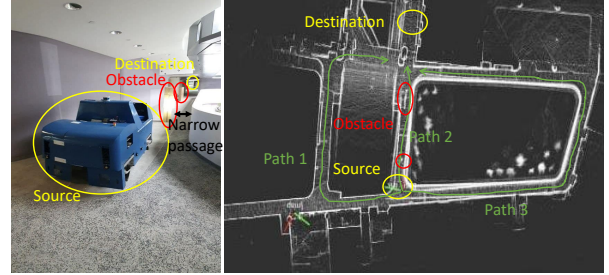


**Figure 13.** The workspace setup of the real environment.

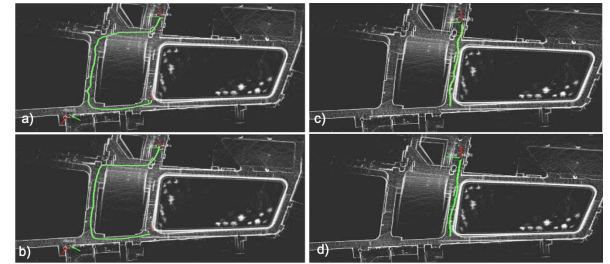


**Figure 14.** The robot navigation trajectories (green color) in the 3D map of the real testbed workspace. (a) RRT\* without reconfiguration, (b) G-RRT\* without reconfiguration, (c) RRT\* with reconfiguration, and (d) G-RRT\* with reconfiguration.

solution paths of G-RRT\* were compared against RRT\* with informed sampling in both SE(2) (i.e., without reconfiguration) and SE(2) +  $\mathbb{R}^2$  state spaces (i.e., with reconfiguration) using the Panthera robot as a case study. Note that G-RRT\* and RRT\* were integrated into Panthera's navigation software stack as the global path planners using the ROS framework (Quigley et al. 2009). To enable the reconfigurable ability, we set the flexible robot base width as the adaptive footprint parameter in the global planning layer. The experiments were conducted for 10 trials, and the solutions of G-RRT\* and RRT\* were selected after 10 seconds of planning time for SE(2) and 30 seconds for SE(2) +  $\mathbb{R}^2$  to conduct the navigation experiments.

Using HDL 3D SLAM (Koide et al. 2018) with a 3D Velodyne 16-channel sensor, the 3D workspace was mapped, as shown in Figure 13. The workspace consists of several possible options (Path 1, 2, and 3, as seen in Figure 13) with different path lengths to connect the predefined source to destination waypoints. Once the global paths were generated to connect these waypoints, the robot followed the path, executing the velocity commands issued by a local trajectory controller to visit the waypoints orderly. The time spent and energy consumption were recorded by Panthera's battery management system after each navigation. The example path

**Table 1.** Execution time and energy consumption of the planners for the real-world testbed environment.

planners	without reconfiguration		with reconfiguration	
	running time (s)	energy consumption (kJ)	running time (s)	energy consumption (kJ)
RRT*	632.25	151.2	372.63	103.6
G-RRT*	592.59	139.9	311.68	92.2

of each tested method is shown in Figure 14. In the case of  $SE(2)$  state space (i.e., a 3-dimensional space without reconfiguration), both RRT\* and G-RRT\* found the solution path through path option 1, and in the case of  $SE(2) + \mathbb{R}^2$  state space (i.e., a 5-dimensional space with reconfiguration), both planners were able to find the path through option 2 with a narrow passage. Nevertheless, the solution paths derived by G-RRT\* within the available time intervals were smoother and had fewer twists and turns than RRT\*.

The average energy consumption and navigation time after 10 trials are presented in Table 1. We can observe that G-RRT\* outperforms RRT\* in terms of both energy usage and time spent, and the margins of outperformance are significantly larger in higher-dimensional state spaces. Specifically, in the case of a 3-dimensional space without reconfiguration, the time and energy spent by RRT\* are only slightly higher than those of the proposed method G-RRT\*, at about 6.69% and 7.47%, respectively. However, when the search space increases to 5 dimensions, considering the reconfiguration of Panthera during planning, RRT\* consumes significantly more time and energy than G-RRT\*, as expected due to the increased complexity in finding optimal solutions. The difference in time and energy consumption for RRT\* in this case increases to 16.35% and 11.01%, respectively, resulting in a trajectory with more turns and less smoothness.

## 7 Conclusion and Discussion

Anytime sampling-based planning algorithms have been proven to perform better in high-dimensional state spaces compared to graph-search approaches since these methods do not explicitly construct high-dimensional occupancy obstacles; instead, they rely on random sampling to asymptotically find optimal solutions. Algorithms like RRT\* increasingly build dense approximations over the problem domain based on randomly sampled states and find continually improving solutions over time. This makes RRT\* probabilistically complete and almost-surely asymptotically optimal (Karaman et al. 2011).

Although they are effective in continuous planning problems, their search is often inefficient since they tend to uniformly explore the entire state space (i.e., they are space-filling algorithms). In other words, these algorithms tend to spend time exploring unnecessary regions of the problem domain where solutions do not exist. This wasted computational effort becomes more pronounced in planning problems with higher dimensions of state space.

Previous works therefore attempt to focus the search solely on promising regions of the problem domain where solutions are likely to exist. Algorithms such as Informed RRT\* directly focus sampling on a subset of the state space

determined by the current solution path. This  $L^2$  informed set contains the set of states that can potentially provide better solutions and often ensures faster convergence guarantees for planning scenarios aimed at minimizing path lengths. However, since this set is estimated using the cost of the current solution path, it can still result in larger sampling regions, especially when the current solution contains many twists and turns.

This paper presents an alternative version of the informed set, called the  $L^2$  greedy informed set, which is approximated based on the exploited knowledge of the current solution path using the maximum admissible heuristic cost (Section 3). Instead of using the cost of the current solution as an admissible heuristic for the informed set, the greedy informed set only considers the maximum heuristic cost within the current solution path. This results in smaller informed subsets and is shown to have better convergence properties than the informed set, typically in problems with complex initial solution paths.

While direct informed sampling techniques prove effective compared to traditional space-filling approaches, their effectiveness only manifests once an initial solution is found. Consequently, the benefits of focused sampling become irrelevant in complex planning problems where finding an initial solution is challenging, especially in high-dimensional state spaces. Hence, finding a fast initial solution is crucial for sampling-based planning algorithms to leverage all the benefits of informed sets. This paper also presents an algorithm that leverages bi-directional search to accelerate the process of finding initial solutions.

To this end, this paper presents an almost-surely asymptotically optimal path planning algorithm that utilizes greedy heuristic techniques to address challenges in high-dimensional planning domains (Section 4). G-RRT\* maintains two rapidly growing random geometric graphs (RGGs) to explore the problem state space and uses a greedy connection heuristic to guide the trees toward each other. This helps G-RRT\* find faster initial solutions and often escape local minima with biased Voronoi regions.

G-RRT\* also focuses the search on the  $L^2$  greedy informed set once the initial solution is found, i.e., forward and reverse search trees meet each other. This allows G-RRT\* to search efficiently on the smaller subset of the problem domain with exploited knowledge the current solution path. Moreover, a greedy biasing ratio is introduced to balance uniform sampling from the problem domain (i.e., exploration with  $L^2$  informed set) for optimal guarantees and path-biased sampling (i.e., exploitation with  $L^2$  greedy informed set) for accelerating convergence. As a result, G-RRT\* is probabilistically complete and almost-surely asymptotically optimal (Section 5).

The benefits of the greedy heuristic techniques are demonstrated on abstract planning problems, manipulation problems in simulations, and real-world trials with a self-reconfigurable robot, Panthera, across a range of dimensions (Section 6). The results from the experiments show that G-RRT\* outperforms all the tested state-of-the-art asymptotically optimal planners, especially in high-dimensional problems. It often searches for faster initial solutions and finds better solutions with a faster convergence rate for problems seeking to minimize path length.

Since the approximation and search of G-RRT\* are based on a single sample per iteration, further research interest lies in extending the idea of greedy informed sampling to batches of randomly generated samples, such as Batch Informed Trees (BIT\*) (Gammell et al. 2020). Additionally, instead of relying solely on static information state spaces, we intend to develop an online version of the geometric path planner that also considers environmental changes in practical, real-world scenarios.

Information on the OMPL implementations of G-RRT\* will be publicly made available at <https://github.com/mlsdpk/ompl>.

## 8 Acknowledgement

This research is supported by the National Robotics Programme under its National Robotics Programme (NRP) BAU, Ermine III: Deployable Reconfigurable Robots, Award No. M22NBK0054 and also, it is supported by the National Robotics Programme under its National Robotics Programme (NRP) BAU, PANTHERA 2.0: Deployable Autonomous Pavement Sweeping Robot through Public Trials, Award No. M23NBK0065.

## References

- Akgun B and Stilman M (2011) Sampling heuristics for optimal motion planning in high dimensions. In: *2011 IEEE/RSJ international conference on intelligent robots and systems*. IEEE, pp. 2640–2645.
- Alterovitz R, Patil S and Derbakova A (2011) Rapidly-exploring roadmaps: Weighing exploration vs. refinement in optimal motion planning. In: *2011 IEEE International Conference on Robotics and Automation*. IEEE, pp. 3706–3712.
- Arslan O and Tsiotras P (2013) Use of relaxation methods in sampling-based algorithms for optimal motion planning. In: *2013 IEEE International Conference on Robotics and Automation*. IEEE, pp. 2421–2428.
- Bialkowski J, Otte M and Frazzoli E (2013) Free-configuration biased sampling for motion planning. In: *2013 IEEE/RSJ International Conference on Intelligent Robots and Systems*. IEEE, pp. 1272–1279.
- Diankov R (2010) *Automated construction of robotic manipulation programs*. PhD Thesis, Carnegie Mellon University, USA.
- Dijkstra EW et al. (1959) A note on two problems in connexion with graphs. *Numerische mathematik* 1(1): 269–271.
- Dobson A and Bekris KE (2014) Sparse roadmap spanners for asymptotically near-optimal motion planning. *The International Journal of Robotics Research* 33(1): 18–47.
- Elbanhawi M and Simic M (2014) Sampling-based robot motion planning: A review. *Ieee access* 2: 56–77.
- Ferguson D and Stentz A (2006) Anytime rrts. In: *2006 IEEE/RSJ International Conference on Intelligent Robots and Systems*. IEEE, pp. 5369–5375.
- Gammell JD, Barfoot TD and Srinivasa SS (2018) Informed sampling for asymptotically optimal path planning. *IEEE Transactions on Robotics* 34(4): 966–984.
- Gammell JD, Barfoot TD and Srinivasa SS (2020) Batch informed trees (bit\*): Informed asymptotically optimal anytime search. *The International Journal of Robotics Research* 39(5): 543–567.
- Gammell JD, Srinivasa SS and Barfoot TD (2014) Informed rrt\*: Optimal sampling-based path planning focused via direct sampling of an admissible ellipsoidal heuristic. In: *2014 IEEE/RSJ International Conference on Intelligent Robots and Systems*. IEEE, pp. 2997–3004.
- Gammell JD, Strub MP and Hartmann VN (2022) Planner developer tools (pdt): Reproducible experiments and statistical analysis for developing and testing motion planners. In: *Proceedings of the Workshop on Evaluating Motion Planning Performance (EMPP), IEEE/RSJ International Conference on Intelligent Robots and Systems (IROS)*.
- Hart PE, Nilsson NJ and Raphael B (1968) A formal basis for the heuristic determination of minimum cost paths. *IEEE transactions on Systems Science and Cybernetics* 4(2): 100–107.
- Hayat AA, Parween R, Elara MR, Parsuraman K and Kandasamy PS (2019) Panthera: Design of a reconfigurable pavement sweeping robot. In: *International Conference on Robotics and Automation (ICRA)*. IEEE, pp. 7346–7352.
- Hsu D, Kavraki LE, Latombe JC, Motwani R, Sorkin S et al. (1998) On finding narrow passages with probabilistic roadmap planners. In: *Robotics: the algorithmic perspective: 1998 workshop on the algorithmic foundations of robotics*. pp. 141–154.
- Islam F, Nasir J, Malik U, Ayaz Y and Hasan O (2012) Rrt\*-smart: Rapid convergence implementation of rrt\* towards optimal solution. In: *2012 IEEE international conference on mechatronics and automation*. IEEE, pp. 1651–1656.
- Jeong IB, Lee SJ and Kim JH (2019) Quick-rrt\*: Triangular inequality-based implementation of rrt\* with improved initial solution and convergence rate. *Expert Systems with Applications* 123: 82–90.
- Jiang H, Chen Q, Zheng Y and Xu Z (2020) Informed rrt\* with adjoining obstacle process for robot path planning. In: *2020 IEEE 20th International Conference on Communication Technology (ICCT)*. IEEE, pp. 1471–1477.
- Karaman S and Frazzoli E (2011) Sampling-based algorithms for optimal motion planning. *The international journal of robotics research* 30(7): 846–894.
- Karaman S, Walter MR, Perez A, Frazzoli E and Teller S (2011) Anytime motion planning using the rrt. In: *2011 IEEE International Conference on Robotics and Automation*. IEEE, pp. 1478–1483.
- Kavraki LE, Svestka P, Latombe JC and Overmars MH (1996) Probabilistic roadmaps for path planning in high-dimensional configuration spaces. *IEEE transactions on Robotics and Automation* 12(4): 566–580.
- Khatib O (1986) Real-time obstacle avoidance for manipulators and mobile robots. *The international journal of robotics research* 5(1): 90–98.
- Kim D, Lee J and Yoon Se (2014) Cloud rrt: Sampling cloud based rrt. In: *2014 IEEE International Conference on Robotics and Automation (ICRA)*. IEEE, pp. 2519–2526.
- Kim MC and Song JB (2015) Informed rrt\* towards optimality by reducing size of hyperellipsoid. In: *2015 IEEE International Conference on Advanced Intelligent Mechatronics (AIM)*. IEEE, pp. 244–248.
- Klemm S, Oberländer J, Hermann A, Roennau A, Schamm T, Zollner JM and Dillmann R (2015) Rrt-connect: Faster, asymptotically optimal motion planning. In: *2015 IEEE international*

- conference on robotics and biomimetics (ROBIO). IEEE, pp. 1670–1677.
- Koide K, Miura J and Menegatti E (2018) A portable 3d lidar-based system for long-term and wide-area people behavior measurement. *IEEE Trans. Hum. Mach. Syst.*
- Kuffner JJ and LaValle SM (2000) Rrt-connect: An efficient approach to single-query path planning. In: *Proceedings 2000 ICRA. Millennium Conference. IEEE International Conference on Robotics and Automation. Symposia Proceedings (Cat. No. 00CH37065)*, volume 2. IEEE, pp. 995–1001.
- LaValle SM (2006) *Planning algorithms*. Cambridge university press.
- LaValle SM and Kuffner Jr JJ (2001) Randomized kinodynamic planning. *The international journal of robotics research* 20(5): 378–400.
- Li Y, Wei W, Gao Y, Wang D and Fan Z (2020) Pq-rrt\*: An improved path planning algorithm for mobile robots. *Expert systems with applications* 152: 113425.
- Liao B, Wan F, Hua Y, Ma R, Zhu S and Qing X (2021) F-rrt\*: An improved path planning algorithm with improved initial solution and convergence rate. *Expert Systems with Applications* 184: 115457.
- Mashayekhi R, Idris MYI, Anisi MH, Ahmedy I and Ali I (2020) Informed rrt\*-connect: An asymptotically optimal single-query path planning method. *IEEE Access* 8: 19842–19852.
- Otte M and Correll N (2013) C-forest: Parallel shortest path planning with superlinear speedup. *IEEE Transactions on Robotics* 29(3): 798–806.
- Pan J, Chitta S and Manocha D (2012) Fcl: A general purpose library for collision and proximity queries. In: *2012 IEEE International Conference on Robotics and Automation*. IEEE, pp. 3859–3866.
- Quigley M, Conley K, Gerkey B, Faust J, Foote T, Leibs J, Wheeler R and Ng AY (2009) Ros: an open-source robot operating system. In: *ICRA workshop on open source software*, volume 3. Kobe, Japan, p. 5.
- Qureshi AH and Ayaz Y (2016) Potential functions based sampling heuristic for optimal path planning. *Autonomous Robots* 40: 1079–1093.
- Reif JH (1979) Complexity of the mover's problem and generalizations. In: *20th Annual Symposium on Foundations of Computer Science (sfcs 1979)*. IEEE Computer Society, pp. 421–427.
- Salzman O and Halperin D (2016) Asymptotically near-optimal rrt for fast, high-quality motion planning. *IEEE Transactions on Robotics* 32(3): 473–483.
- Strub MP and Gammell JD (2020) Adaptively informed trees (ait\*): Fast asymptotically optimal path planning through adaptive heuristics. In: *2020 IEEE International Conference on Robotics and Automation (ICRA)*. IEEE, pp. 3191–3198.
- Strub MP and Gammell JD (2022) Adaptively informed trees (ait\*) and effort informed trees (eit\*): Asymmetric bidirectional sampling-based path planning. *The International Journal of Robotics Research* 41(4): 390–417.
- Sucan IA, Moll M and Kavraki LE (2012) The open motion planning library. *IEEE Robotics & Automation Magazine* 19(4): 72–82.
- Wang J, Chi W, Li C, Wang C and Meng MQH (2020a) Neural rrt\*: Learning-based optimal path planning. *IEEE Transactions on Automation Science and Engineering* 17(4): 1748–1758.
- Wang J, Chi W, Shao M and Meng MQH (2019) Finding a high-quality initial solution for the rrts algorithms in 2d environments. *Robotica* 37(10): 1677–1694.
- Wang J, Li CXT, Chi W and Meng MQH (2018) Tropicistic rrt: An efficient planning algorithm via adaptive restricted sampling space. In: *2018 IEEE International Conference on Information and Automation (ICIA)*. IEEE, pp. 1639–1646.
- Wang J, Li T, Li B and Meng MQH (2022) Gmr-rrt\*: Sampling-based path planning using gaussian mixture regression. *IEEE Transactions on Intelligent Vehicles* 7(3): 690–700.
- Wang Z, Li Y, Zhang H, Liu C and Chen Q (2020b) Sampling-based optimal motion planning with smart exploration and exploitation. *IEEE/ASME Transactions on Mechatronics* 25(5): 2376–2386.
- Yershova A, Jaillet L, Siméon T and LaValle SM (2005) Dynamic-domain rrts: Efficient exploration by controlling the sampling domain. In: *Proceedings of the 2005 IEEE international conference on robotics and automation*. IEEE, pp. 3856–3861.
- Zhang T, Wang J and Meng MQH (2021) Generative adversarial network based heuristics for sampling-based path planning. *IEEE/CAA Journal of Automatica Sinica* 9(1): 64–74.